Transworld Research Network
37/661 (2), Fort P.O., Trivandrum-695 023, Kerala, India

Gas Phase Molecular Reaction and Photodissociation Dynamics, 2007: 113-159
ISBN: 978-81-7895-305-2 Editors: K.C. Lin and P.D. Kleiber

3

Theoretical studies of potential energy surfaces and product branching ratios for the reactions of C_2 with small unsaturated hydrocarbons (acetylene, ethylene, methylacetylene, and allene)

A. M. Mebel[1], V. V. Kislov[1] and R. I. Kaiser[2]
[1]Department of Chemistry and Biochemistry, Florida International University Miami, FL 33199, USA; [2]Department of Chemistry, University of Hawai'i at Manoa, Honolulu, HI 96822-2275, USA

1. Introduction

The dicarbon molecule, $C_2(X^1\Sigma_g^+)$, is ubiquitous in various environments and has been detected in hydrocarbon flames, in chemical vapor deposition of diamond, and in the interstellar medium, including

Correspondence/Reprint request: Dr. A. M. Mebel, Department of Chemistry and Biochemistry, Florida International University, Miami, FL 33199, USA. E-mail: mebela@fiu.edu

cold molecular clouds, circumstellar envelopes, and cometary comae. Therefore, the reaction dynamics and energetics of dicarbon with unsaturated hydrocarbons are important for understanding combustion processes [1-4] and the chemical evolution of extraterrestrial environments such as molecular clouds and circumstellar envelopes of dying carbon stars [5-10]. Reactions of the C_2 in its $X^1\Sigma_g^+$ electronic ground and first electronically excited $a^3\Pi_u$ state are of particular interest in untangling the formation of polycyclic aromatic hydrocarbons (PAHs), their hydrogen deficient precursors, and of carbon-rich nanostructures up to fullerenes from the 'bottom up' [11-16]. Synthetic routes are proposed via sequential addition steps of ground-state atomic carbon, carbon molecules (C_2 and C_3) and small hydrocarbon radicals to unsaturated hydrocarbons eventually leading to PAH-like structures and fullerenes. The reactions of C_2 may open prompt routes to form hydrocarbon radicals with multiple carbon-carbon bonds, including resonance-stabilized free radicals (RSFRs) such as C_4H, C_4H_3, and C_5H_3. These radicals are believed to play an important role in the formation of aromatic compounds, PAHs, and soot in the combustion of aromatic fuels. Thus, understanding of the C_2 reactions with unsaturated hydrocarbons should be helpful in unraveling the formation mechanisms of RSFRs in flames and in the interstellar media.

Due to this importance, the kinetics of dicarbon reactions has been extensively investigated at room temperature [17-23] (recall that the electronically excited triplet state, $a^3\Pi_u$, lies only 718.32 cm^{-1} above the ground state $X^1\Sigma_g^+$). The disappearance of dicarbon in the two electronic states ($X^1\Sigma_g^+$ and $a^3\Pi_u$) was followed in these studies; the reactions of $C_2(X^1\Sigma_g^+)$ were found to be fast (of the gas kinetic order when the molecular partner is an unsaturated hydrocarbon), whereas the $C_2(a^3\Pi_u)$ reactions were suggested to be systematically slower. However, despite these extensive kinetic studies, information on the products of dicarbon reactions together with the intermediates involved is still lacking. In some cases, primary products and reaction mechanisms were speculated on the basis of the observed temperature dependence of the reactions. For instance, from the measured removal rate constants of $C_2(X^1\Sigma_g^+)$ and $C_2(a^3\Pi_u)$ by ethylene, the favored approach was suggested to be an addition of the electrophilic C_2 (both singlet and triplet states) to the olefinic π bond. Nevertheless, $C_2(X^1\Sigma_g^+)$ reacts faster than $C_2(a^3\Pi_u)$. This implies that $C_2(X^1\Sigma_g^+)$ could also react through some alternative pathways. A few reactions of dicarbon were also investigated at 10 K and 77 K in the condensed phase and via ab initio calculations in order to understand the reaction mechanism [24]. Interestingly, the reaction products of the reaction of dicarbon with ethylene have been always speculated to be C_2H and C_2H_3 (Δ_rH = –8.8 kcal mol^{-1} or C_2H_2 and C_2H_2 (Δ_rH = –104.2 kcal mol^{-1}) – so far without any experimental confirmation. These considerations make it clear that novel

laboratory and theoretical studies on reactions of dicarbon with unsaturated hydrocarbons which provide reaction products, their branching ratios, the intermediates involved, and the thermodynamic properties of product isomers - data which kinetic measurements cannot supply - are required.

The research program in our groups is aimed to address these issues through a combination of experimental measurements of C_2 reactions in crossed molecular beams with theoretical electronic structure calculations of their potential energy surfaces. In particular, crossed molecular beam experiments at the University of Hawaii focus on the collision-energy dependent reaction dynamics of dicarbon molecules with unsaturated hydrocarbons, such as acetylene ($C_2H_2(X^1\Sigma_g^+)$), ethylene ($C_2H_4(X^1A_g)$), methylacetylene ($CH_3CCH(X^1A_1)$), and allene (H_2CCCH_2 (X^1A_1)) [25]. These systems represent prototype reactions of ubiquitous interstellar dicarbon molecules with hydrocarbons to synthesize hydrocarbon radicals via a single neutral-neutral collision in the outflow of carbon rich AGB stars and in cold molecular clouds. Specifically, the closed shell hydrocarbon molecules serve as model reactants with triple (acetylene) and double (ethylene) bonds; methylacetylene and allene are chosen as the simplest representatives of closed shell hydrocarbon species to investigate how the chemical reaction dynamics change from one structural isomer to the other. Since all chemical processes in cold molecular clouds and circumstellar envelopes consist of multiple elementary reactions that are a series of bimolecular encounters, for instance, between dicarbon molecules and hydrocarbons, a detailed knowledge of the elementary processes involved at the most fundamental, microscopic level under single collision conditions is truly imperative. This means that in a bimolecular reaction of a dicarbon molecule with an unsaturated hydrocarbon, one carbon cluster reacts with only one hydrocarbon molecule without collisional stabilization and/or successive reaction of the potential reaction intermediate(s). The primary reaction products are expected to be highly hydrogen deficient carbon bearing molecules, such as, for example, in the C_2 for H exchange channel, $C_nH_m + C_2 \rightarrow C_{n+2}H_{m-1} + H$. However, other reaction products are also possible in principle and cannot be arbitrarily ruled out. The goal of our theoretical studies described in this Chapter is to reveal the detailed reaction mechanism through calculations of potential energy surfaces (PES), to predict chemically accurate energetics and molecular properties of potential intermediates, transition states, and reaction products, and to evaluate reaction rate constants and product branching ratios depending on the collision energy, if the reactions take place statistically and follow RRKM behavior.

This Chapter is organized as follows. After describing the general theoretical approach and methods used in calculations (Section 2), we address the reactions of C_2 with acetylene (Section 3), ethylene (Section 4), methylacetylene (Section 5), and allene (Section 6). Each section depicts both

singlet (relevant to the reactions of $C_2(^1\Sigma_g^+)$) and triplet (for the $C_2(^3\Pi_u)$ reactions) PES and results of RRKM calculations of energy-dependent reaction rate constants and product branching ratios. In the end of each Section, we compare our results and conclusions with available experimental observations. Finally, general conclusions and implications of our findings to combustion and interstellar chemistry are given in Chapter 7.

2. Theoretical approach and methods

A theoretical study of kinetics and dynamics for elementary chemical reactions requires careful investigation of PESs, because they determine how the nuclei in molecules move, break chemical bonds, and create new bonds during the reaction. Because of the great progress achieved in the field of computational chemistry in recent years, it is now feasible to perform calculations of PESs for the reactions between small and medium-size molecules to chemical accuracy (within 1-2 kcal mol^{-1}) using advanced methods of quantum chemistry. For the reactions described in this Chapter, PES calculations started from a search of transition states (TS) for $C_2(^1\Sigma_g^+/^3\Pi_u)$ additions to various sites of their reaction counterparts to form initial intermediates. If an appropriate distinct transition state could not be found, to confirm that it does not exist we performed a scan of PES in the entrance reaction channel, i.e., partial geometry optimization using the distance between the attacking dicarbon molecule and an unsaturated hydrocarbon as a parameter, which was fixed at certain values as the reactants approach each other. After the entrance channel and the initial reaction intermediates were characterized, the calculations proceeded through a variety of intramolecular rearrangements (hydrogen atom migrations, ring openings and closures, conformational changes), and were completed by finding all probable fragmentation channels, including hydrogen atom eliminations, ruptures of carbon-carbon bonds leading to radical products, and splitting of closed-shell molecules (e.g. H_2, C_2H_2, CH_4 elimination). We also searched for transition states for direct hydrogen atom abstraction channels. Thus, all relevant local minima and TS on the surfaces were mapped out.

The geometries of the reactants, products, intermediates, and transition states have been optimized at the hybrid density functional B3LYP level of theory [26,27] with the 6-311G(d,p) basis set. Vibrational frequencies have been calculated at the same level and were used for characterization of the stationary points as local minima or transition states, to compute zero-point energy corrections (ZPE), and for statistical calculations of rate constants for individual reactions steps. The connections between transition states and corresponding intermediates have been confirmed by intrinsic reaction coordinate (IRC) [28] calculations at the B3LYP/6-311G(d,p) level. To refine

relative energies of various species, we employed the G2M(RCC,MP2) computational procedure [29], which approximates coupled cluster RCCSD(T) energy [30-33] with the large 6-311+G(3df,2p) basis set. The G2M(RCC,MP2)//B3LYP/6-311G(d,p)+ZPE[B3LYP/6-311G(d,p)] calculational approach normally provides accuracy of 1-2 kcal mol^{-1} for relative energies of various stationary points on PES including transition states, unless a wave function has a strong multireference character. The closed-shell singlet wave functions of key intermediates and transition states were tested on the subject of their instability with respect to an open-shell character. Where necessary, geometry optimization and vibrational frequency calculations were performed at the multireference complete-active-space self-consistent field CASSCF level [34,35] and single-point energies were then recalculated at the more accurate CASPT2/6-311+G(3df,2p) level [36], which takes into account dynamic correlation. For the C_2 + C_2H_2 system, single-point calculations of energies were carried out at the RCCSD(T)/6-311+G(3df,2p) level of theory. The GAUSSIAN 98 [37], MOLPRO 2002 [38], and DALTON [39] program packages were employed for the calculations.

We used RRKM theory for computations of rate constants of individual reaction steps [40-42]. Rate constant k(E) at an internal energy E for a unimolecular reaction $A^* \rightarrow A^{\#} \rightarrow P$ can be expressed as

$$k(E) = \frac{\sigma}{h} * \frac{W^{\neq}(E - E^{\neq})}{\rho(E)}$$

where σ is the reaction path degeneracy, h is Plank's constant, $W^{\#}(E\text{-}E^{\#})$ denotes the total number of states for the transition state (activated complex) $A^{\#}$ with a barrier $E^{\#}$, ρ(E) represents the density of states of the energized reactant molecule A*, and P is the product or products. The calculations were performed at different values of the internal energy E computed as a sum of the energy of chemical activation (the relative energy of an intermediate or a transition state with respect to the initial reactants) and the collision energy E_{col}.

For the reaction channels, which do not exhibit exit barriers, such as those occurring by a cleavage of single C-H or C-C bonds, we applied the microcanonical variational transition state theory (VTST) [42] and thus determined variational transition states and rate constants. In microcanonical VTST, the minimum in the microcanonical rate constant is found along the reaction path according to the following equation

$$\frac{dk(E)}{dq^{\#}} = 0,$$

where $q^{\#}$ is the reaction coordinate (for instance, the length of the breaking C-H bond), so that a different transition state is found for each different energy. The individual microcanonical rate constants were minimized at the point along the reaction path where the sum of states $W^{\#}(E-E^{\#})$ has a minimum. Each of these calculations requires values of the classical potential energy, zero-point energy, and vibrational frequencies as functions of the reaction coordinate. 3N – 7 vibrational frequencies projected out of the gradient direction were computed along the minimal energy reaction path for these purposes.

Assuming single-collision conditions for the reaction, kinetic equations for unimolecular reactions can be expressed as follows:

$$\frac{d[C]_i}{dt} = \sum k_n [C]_j - \sum k_m [C]_i$$

where $[C]_i$ and $[C]_j$ are concentrations of various intermediates or products, k_n and k_m are microcanonical rate constants computed using the RRKM theory. Only a single total-energy level was considered throughout, as for single-collision crossed-beam conditions. We used the steady-state approximation to solve the system of kinetic equations and to compute the product branching ratios. Alternatively, in order see how the concentrations change with time, we used the fourth-order Runge-Kutta method to solve the equations; the product concentrations at the time when they converged were then used to compute branching ratios. The branching ratios obtained using these two different approaches are usually nearly identical.

3. Reactions of C_2 with acetylene

3.1. $C_2(^1\Sigma_g^+)$ + $C_2H_2(^1\Sigma_g^+)$: Singlet potential energy surface

According to the calculated PES of the C_2 + acetylene reaction in the ground singlet electronic state shown in Figure 1, the reaction starts by barrierless addition of the dicarbon molecule to the triple C≡C bond of C_2H_2 in either end-on or side-on manner. If the addition occurs perpendicularly to the C≡C bond (end-on), a three-member ring C_{2v}-symmetric intermediate **ac-s1** is produced with the energy gain of 68.9 kcal mol^{-1}. The parallel (side-on) addition leads to a four-member ring structure **ac-s2** residing 68.1 kcal mol^{-1} below the reactants. The ring in **ac-s2** is not planar and this intermediate possesses only C_2 symmetry. The two initial adducts can readily transform to one another overcoming a relatively low barrier of 15.7 (14.9) kcal mol^{-1} for the ring expansion (contraction). At the subsequent reaction step, the four-member ring isomer **ac-s2** undergoes ring opening over a barrier of 21.2 kcal mol^{-1} to form diacetylene, HCCCCH **ac-s3**. The ring opening process in **ac-s2**

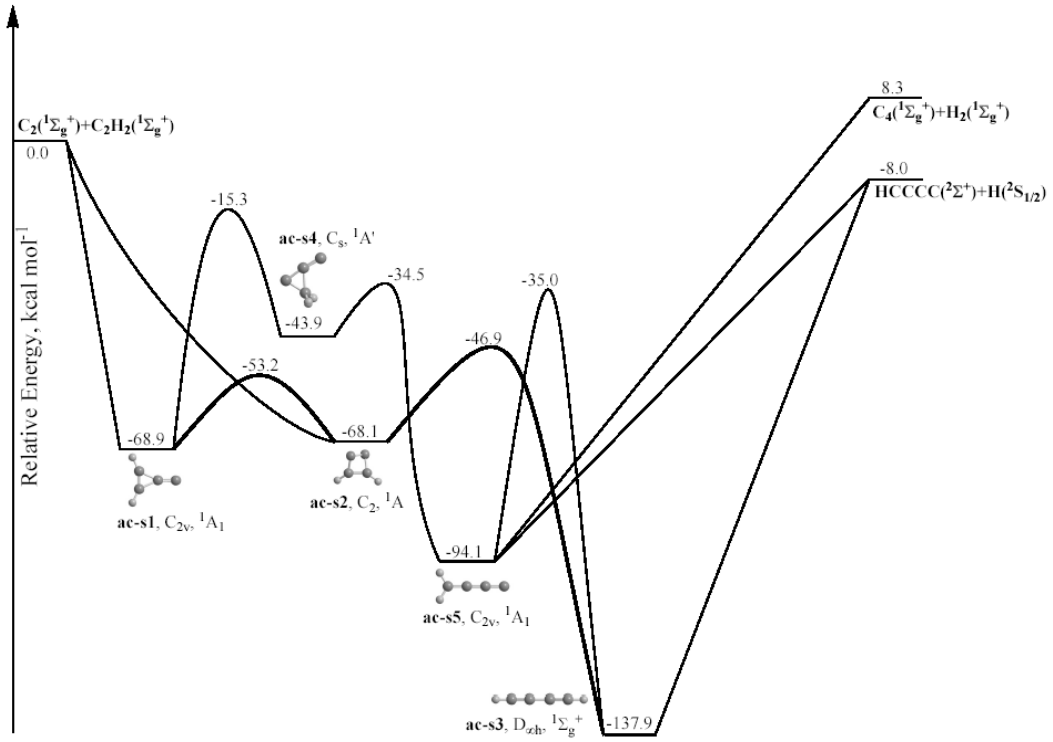

Figure 1. Potential energy diagram of the $C_2(^1\Sigma_g^+) + C_2H_2(^1\Sigma_g^+)$ reaction.

is rather peculiar. The HC-CH bond is not cleaved directly to produce diacetylene. Instead, according to intrinsic reaction coordinate calculations, one of the dicarbon atoms formally inserts between two acetylene carbon atoms, and the second takes the terminal position in the C_4 chain. This is followed by a spontaneous hydrogen shift to this terminal carbon. Therefore, when $C_2(^1\Sigma_g^+)$ attacks isotopically labeled $^{13}C_2H_2(^1\Sigma_g^+)$, the $H^{13}CC^{13}CCH$ diacetylene isotopomer should be produced after the ring opening process.

Diacetylene **ac-s3** resides in a deep potential well of 137.9 kcal mol^{-1} relative to the reactants and is the most stable isomer of singlet C_4H_2. H elimination from diacetylene gives the final reaction product, 1,3-butadiynyl radical C_4H ($X^2\Sigma^+$). The H loss process from **ac-s3** takes place without an exit barrier, as it corresponds to a single C-H bond cleavage, and is calculated to be endothermic by 129.9 kcal mol^{-1}. Overall, the C_4H ($X^2\Sigma^+$) + H products are 8.0 kcal mol^{-1} lower in energy than the $C_2(^1\Sigma_g^+) + C_2H_2(^1\Sigma_g^+)$ reactants.

An alternative three-step pathway from **ac-s1** to **ac-s3** also exists. It starts from a 1,2-H shift in **ac-s1** to form another three-member ring intermediate **ac-s4** (43.9 kcal mol^{-1} below the reactants) with two hydrogen atoms attached to one of the ring carbon atoms. However, the barrier for the H migration is high, 53.6 kcal mol^{-1} relative to **ac-s1**. Then, **ac-s4** undergoes ring opening leading to a chain C_{2v}-symmetric intermediate **ac-s5**, H_2CCCC (94.1 kcal mol^{-1} lower

in energy than $C_2(^1\Sigma_g^+)$ + $C_2H_2(^1\Sigma_g^+)$), over a low barrier of 9.4 kcal mol^{-1}. H_2CCCC can lose an H atom producing C_4H ($X^2\Sigma^+$) + H without an exit barrier or can be subjected to a 1,4-H migration to form diacetylene **ac-s3** with a barrier of 59.1 kcal mol^{-1}. The H_2CCCC intermediate is also a precursor of the $C_4(a^1\Sigma_g^+)$ + H_2 products. According to the minimal energy path calculations from **ac-s5** to $C_4(a^1\Sigma_g^+)$ + H_2, the H_2 elimination occurs without an exit barrier. However, this process is highly endothermic (by 102.4 kcal mol^{-1}) and the $C_4(a^1\Sigma_g^+)$ + H_2 products reside 8.3 kcal mol^{-1} above the initial reactants.

On the basis of the calculated singlet PES for the $C_2(^1\Sigma_g^+)$ + $C_2H_2(^1\Sigma_g^+)$ reaction, we can conclude that under single collision conditions, C_4H ($X^2\Sigma^+$) + H should be the dominant, if not exclusive, reaction products and most of them are formed by the H loss from the diacetylene intermediate **ac-s3**. This conclusion is also supported by RRKM calculations of the reaction rate constants, which show that the ratio of rate constants for the **ac-s1** → **ac-s2** (ring expansion) and **ac-s1** → **ac-s4** (H migration) processes is in the range of 4×10^4 at reaction collision energies of 0-12 kcal mol^{-1}. This indicates that the formation of **ac-s5** via **ac-s4** is highly unlikely. Even if a small amount of **ac-s5** can be formed, it is much more likely to decompose to C_4H ($X^2\Sigma^+$) + H rather than to $C_4(a^1\Sigma_g^+)$ + H_2 because of the significant (16.3 kcal mol^{-1}) energy preference of H elimination from H_2CCCC as compared to H_2 elimination. Thus, the dominant reaction mechanism under single collision conditions should be $C_2(^1\Sigma_g^+)$ + $C_2H_2(^1\Sigma_g^+)$ → **ac-s1** (or **ac-s2**) → **ac-s2** → HCCCCH (**ac-s3**) → C_4H ($X^2\Sigma^+$) + H.

3.2. $C_2(^3\Pi_u)$ + $C_2H_2(^1\Sigma_g^+)$: Triplet potential energy surface

Three different triplet C_4H_2 isomers can be formed at the initial reaction step (Figure 2). Symmetric addition of dicarbon to the center of the acetylenic bond gives C_{2v}-symmetric three-member ring intermediate **ac-t1**, a triplet analog of singlet **ac-s1**, which lies 39.2 kcal mol^{-1} below $C_2(^3\Pi_u)$ + $C_2H_2(^1\Sigma_g^+)$. Alternatively, asymmetric C_2 addition to one of the carbon atoms of acetylene can lead to *cis* and *trans* HCC(H)CC chain intermediates **ac-t2** and **ac-t3**, 42.3 and 43.0 kcal mol^{-1} lower in energy than the reactants, respectively. All three addition processes exhibit no entrance barriers. **ac-t2** and **ac-t3** can rearrange to one another by rotation around the double HC=CH bond with the barriers of 12.7 and 13.4 kcal mol^{-1}, respectively. Also, **ac-t2** can undergo a ring closure to form the cyclic intermediate **ac-t1** overcoming a similar 12.7 kcal mol^{-1} barrier. Both transition states for rotation and ring closure reside 29.6 kcal mol^{-1} below the initial reactants and so the rearrangements between the three initial adducts should be facile under single collision conditions, where the molecules keep all the chemical activation energy in the form of internal energy and there is no energy dissipation through secondary collisions. H elimination from **ac-t3**

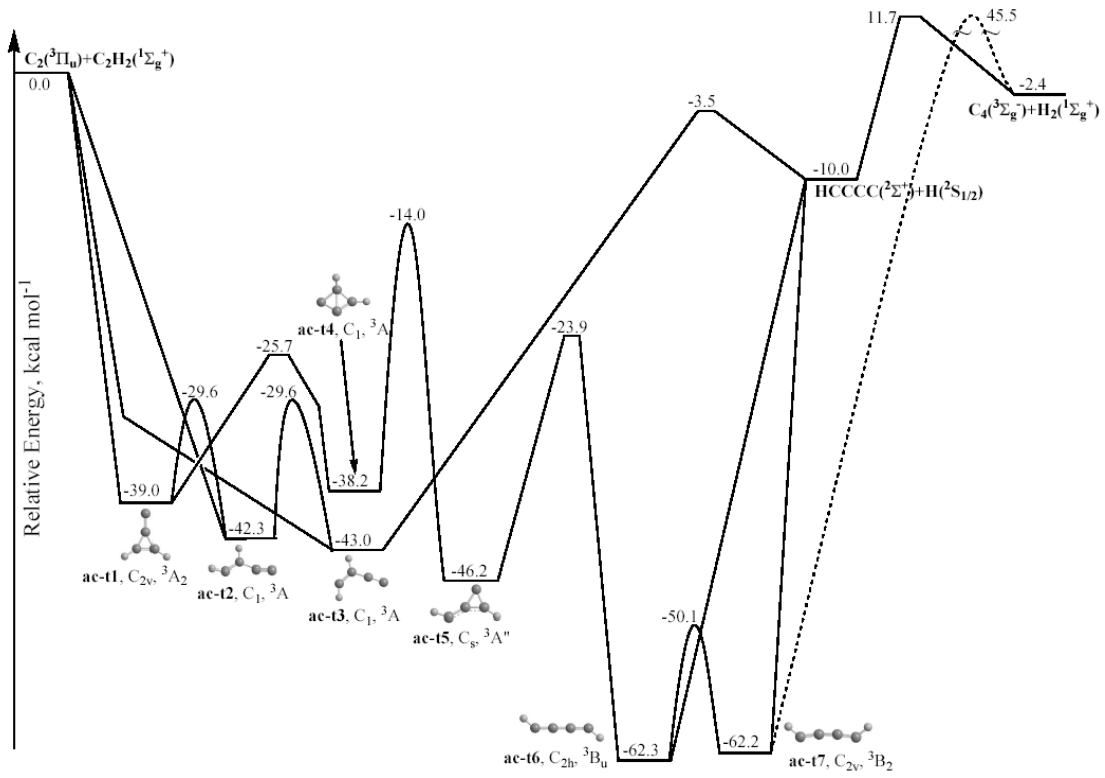

Figure 2. Potential energy diagram of the $C_2(^3\Pi_u) + C_2H_2(^1\Sigma_g^+)$ reaction.

gives the C_4H ($X^2\Sigma^+$) + H products. On the contrary to the singlet PES, this particular H loss channel involves an exit barrier, with the corresponding transition state lying 6.5 kcal mol^{-1} above the products. The existence of the exit barrier can be rationalized in terms of a significant geometry change and hence inherent electron reorganization from the decomposing **ac-t3** intermediate to the 1,3-butadiynyl radical. Here, our computations suggest r(H-C1) = 1.083 Å, r(H-C2) = 1.089 Å, r(C1-C2) = 1.351 Å, r(C2-C3) = 1.388 Å, and r(C3-C4) = 1.279 Å (**ac-t3**) compared to r(H-C1) = 1.063 Å, r(C1-C2) = 1.206 Å, r(C2-C3) = 1.365 Å, and r(C3-C4) = 1.211 Å (1,3-butadiynyl). Although the reversed reaction between 1,3-butadiynyl and atomic hydrogen presets formally an atom-radical reaction, this reaction does not portray a simple recombination of two radical centers as found on the singlet surface, but rather an addition of the hydrogen atom to a carbon-carbon triple bond of the 1,3-butadiynyl radical. Noteworthy, in a related system, a similar barrier of 4.7 kcal mol^{-1} was found for the addition of atomic hydrogen to the carbon-carbon triple bond of acetylene, $C_2H_2(X^1\Sigma_g^+)$ [43].

Rearrangements of the cyclic adduct **ac-t1** can eventually lead to the most stable triplet C_4H_2 isomers, two conformations of triplet diacetylene, **ac-t6** and **ac-t7**. The pathway starts with a second ring closure in **ac-t1**, which exhibits a barrier of 13.3 kcal mol^{-1} and leads to a bicyclic intermediate **ac-t4** residing

38.2 kcal mol^{-1} below the reactants. At the next step, one of the two three-member rings in **ac-t4** opens up to form another three-member ring isomer **ac-t5** featuring an out-of-ring CH group. The calculated barrier between **ac-t4** and **ac-t5** is higher, 24.2 kcal mol^{-1}, and **ac-t5** is 46.2 kcal mol^{-1} lower in energy than $C_2(^3\Pi_u)$ + $C_2H_2(^1\Sigma_g^+)$. Finally, three-member ring opening in **ac-t5** results in the chain HCCCCH structure of triplet *trans*-diacetylene **ac-t6** over a barrier of 22.3 kcal mol^{-1}. **ac-t6** features a linear C_4 skeleton and possesses C_{2h} symmetry. It can isomerize to triplet *cis*-diacetylene **ac-t7** of C_{2v} symmetry by in-plane scrambling of an H atom with a barrier of 12.2 kcal mol^{-1}. **ac-t6** and **ac-t7** are nearly isoergic and lie 62.3 and 62.2 kcal mol^{-1} below the reactants. Both HCCCCH isomers can lose a hydrogen atom to form the C_4H ($X^2\Sigma^+$) + H products with endothermicity of ~52 kcal mol^{-1} but without exit barriers. In this case, the reverse C_4H ($X^2\Sigma^+$) + H $\rightarrow$ **ac-t6**/**ac-t7** reactions occur by H addition to the radical site of the 1,3-butadiynyl radical and are significantly more exothermic than the H addition to the triple bond of C_4H ($X^2\Sigma^+$), C_4H ($X^2\Sigma^+$) + H $\rightarrow$ **ac-t3**. The combination of these two factors is responsible for the fact that the formation of HCC(H)CC **ac-t3** in the reaction of 1,3-butadiynyl with H atoms shows a barrier (6.5 kcal mol^{-1}), whereas the formation of the HCCCCH structures **ac-t6** and **ac-t7** is barrierless.

We can see that the C_4H + H products can be formed in the $C_2(^3\Pi_u)$ + $C_2H_2(^1\Sigma_g^+)$ reaction by two competitive mechanisms, (**ac-t1** $\rightarrow$ **ac-t2** $\rightarrow$) **ac-t3** $\rightarrow$ C_4H + H and **ac-t1** $\rightarrow$ **ac-t4** $\rightarrow$ **ac-t5** $\rightarrow$ **ac-t6** $\rightarrow$ (**ac-t7** $\rightarrow$) C_4H + H. The most significant difference between the two is the existence of a 6.5 kcal mol^{-1} exit barrier for the former and the absence of such a barrier in the latter. Kinetically, the pathway via the triplet diacetylene structures is clearly preferable if the reaction follows a statistical behavior. However, if the lifetime of the triplet C_4H_2 intermediates in the reaction is not sufficient for the complete intramolecular vibrational redistribution (IVR), the mechanism involving the H loss from **ac-t3** can significantly contribute, as it represents a more direct process.

We also considered the possibility to eliminate molecular hydrogen on the triplet surface. The $C_4(X^3\Sigma_g^-)$ + $H_2(X^1\Sigma_g^+)$ products lie 2.4 kcal mol^{-1} below the reactants and the potential precursor for H_2 elimination is **ac-t7**. The respective transition state has a six-member ring structure and lies very high in energy, 45.5 kcal mol^{-1} above $C_2(a^3\Pi_u)$ + $C_2H_2(X^1\Sigma_g^+)$ (Figure 2). Thus, the forward and reverse barriers for the H_2 loss from **ac-t7** are 107.7 and 47.9 kcal mol^{-1} and this channel is very unfavorable. If we consider the reverse reaction of $C_4(X^3\Sigma_g^-)$ with molecular hydrogen in terms of 1,1-H_2 addition to a terminal carbon atom, tetracarbon can be looked at as a σ-radical, similar to $C_2H_3(X^2A')$, $C_2H(X^2\Sigma^+)$, or $HCCCC(X^2\Sigma^+)$. It was demonstrated earlier [44-47], on the basis of the molecular orbital consideration, that $H_2(X^1\Sigma_g^+)$ addition

to such σ-radicals is forbidden; such radicals prefer to react with molecular hydrogen by hydrogen abstraction. Our TS search here also converges to an H abstraction transition state connecting C_4H ($X^2\Sigma^+$) + H with $C_4(X^3\Sigma_g^-)$ + H_2 over a barrier of 21.7 kcal mol^{-1}. This makes the reverse reactions of molecular hydrogen elimination unlikely since an atomic hydrogen loss followed by a hydrogen abstraction is preferable. Another possible reaction channel is a direct H abstraction by C_2 from C_2H_2 to form $C_2H(X^2\Sigma^+)$ + $C_2H(X^2\Sigma^+)$, but it is calculated to be endothermic by 19.2 kcal mol^{-1}. The H abstraction barrier in the triplet electronic state is high, 26.3 kcal mol^{-1}, making this channel unlikely. Also, according to our calculations, the direct hydrogen abstraction is not possible in the ground singlet state**,** where the $C_2(X^1\Sigma_g^+)$ addition to the acetylene molecule is a much more favorable process.

3.3. Comparison with experimental crossed molecular beams results

The reaction of dicarbon molecules in their electronic ground singlet and first excited triplet states with acetylene was investigated at different collision energies between 2.5 and 11.4 kcal mol^{-1} under single collision conditions of crossed molecular beams [48,49]. Two reaction microchannels were detected, both leading to the 1,3-butadiynyl radical plus a hydrogen atom. The first microchannel involves the singlet surface, where dicarbon was found to react with acetylene through an indirect reaction mechanism involving a diacetylene intermediate. The latter fragmented via a loose exit transition state by an emission of a hydrogen atom to form the 1,3-butadiynyl radical $C_4H(X^2\Sigma^+)$. The $D_{\infty h}$ symmetry of the decomposing diacetylene intermediate results in collision-energy invariant, isotropic (flat) center-of-mass angular distributions of this microchannel. Isotopic substitution experiments suggested that the diacetylene isotopomers are long-lived with respect to their rotational periods, which is in agreement with our theoretical predictions based on the calculated singlet PES. For the second microchannel, the observed product translational energy distribution points to an existence of an exit barrier of ~4.1 kcal mol^{-1} for the formation of C_4H + H, which closely correlates with the exit barrier calculated for the H loss from the **ac-t3** triplet intermediate. Therefore, some fraction of the products is formed directly from **ac-t3**. On the triplet surface, the reaction involves three feasible addition complexes **ac-t1**, **ac-t2**, and **ac-t3** located in shallower potential energy wells as compared to singlet diacetylene. This could lead to a lifetime shorter than the rotation period of these intermediates and therefore the asymmetry of the center-of-mass angular distributions observed in experiment for the second reaction microchannel can be explained in terms of the involvement of the triplet surface. The detection of the 1,3-butadiynyl radical, $C_4H(X^2\Sigma^+)$, in the crossed beam reaction of

dicarbon molecules with acetylene presented convincing evidence that the 1,3-butadiynyl radical can be formed via bimolecular reactions involving carbon clusters in extreme environments such as circumstellar envelopes of dying carbon stars and combustion flames. No products other than C_4H + H were found experimentally, which also agrees with the results of our theoretical calculations.

The reaction of C_2 with D1-acetylene (HCCD) was also studied experimentally under single collision conditions in crossed molecular beams [50]. One of the goals of this study was to determine the C_4D vs. C_4H branching ratio in the reaction, which is relevant to deuterium enrichment processes in cold molecular clouds and in circumstellar envelopes of carbon stars. The measured C_4D + H / C_4H + D branching ratios were 2.4$\pm$0.3, 2.3$\pm$0.3, 2.4$\pm$0.3, and 2.6$\pm$0.3 at collision energies of 5.2, 6.9, 9.5, and 11.4 kcal mol^{-1}, respectively. We compared these experimental findings with our theoretical results. RRKM calculations of reaction rate constants followed by solving first-order kinetic equations to find the branching ratios were based on the PESs shown in Figs. 1 and 2, where the isotope effects were taken into account through calculations of vibrational frequencies and ZPE corrections for different isotopomers of various intermediates and transition states. We found that on the singlet surface, the unimolecular decomposition of D1-diacetylene (DCCCCH) leads to a deuterium enrichment; as the collision energies rise from 0 to 12 kcal mol^{-1}, the calculated branching ratios of the hydrogen loss versus deuterium loss decrease only slightly from 2.3 to 2.0. On the triplet surface, where we considered only the H/D loss from the **ac-t3** intermediate as the channel believed to be observed experimentally, we found ratios ranging from 5.8 to 2.2 at collision energies between 0 and 12 kcal mol^{-1}, respectively. Therefore, even at collision energies of 12 kcal mol^{-1}, which corresponds formally to temperatures of about 6000 K, a deuterium enrichment in the 1,3-butadiynyl radical is evident. This – to our best knowledge – is the first combined experimental and theoretical evidence that deuterium enrichments are feasible at elevated temperatures up to a few thousand Kelvin. The branching ratios of the hydrogen versus deuterium loss pathways computed at the collision energies 5.2, 6.9, 9.5, and 11.4 kcal mol^{-1} on the singlet and triplet surfaces agree well with the experimental values ranging, within the error limits, from 2.3 to 2.6. Although the relative concentration of triplet versus singlet dicarbon in the experimental beam was not known, the computed branching ratios for the singlet and triplet surfaces are very similar and also in good agreement with the experimental values. In summary, our combined experimental and theoretical studies suggest that the barrierless C_2 + HCCD reaction can induce a deuterium enrichment in the D1-1,3-butadiynyl radial (CCCCD) over a broad range of collision energies formally corresponding to temperatures from 10 K to a few 1,000 K as present in cold

molecular clouds and circumstellar envelopes close to the photosphere, respectively.

4. Reactions of C_2 with ethylene

4.1. $C_2(^1\Sigma_g^+)$ + $C_2H_4(^1A_g)$: Singlet potential energy surface

As seen from the potential energy diagram shown in Figure 3 [51], when a singlet C_2 molecule adds to ethylene, a cyclic planar C_4H_4 intermediate **et-s1** (carbenecyclopropane) is initially produced. The addition occurs without an entrance barrier and is calculated to be 85.5 kcal mol^{-1} exothermic. At the next reaction step, the C_2 fragment inserts into the C-C bond of C_2H_4 over a barrier of 14.2 kcal mol^{-1} to form a much more stable D_{2h}-symmetric butatriene molecule **et-s2**, which resides 132.5 kcal mol^{-1} below the initial reactants. The butatriene intermediate can decompose through three different channels. The first one is elimination of a hydrogen atom leading to the 1-butene-3-yne-2-yl radical [i-$C_4H_3(X^2A')$, H_2CCCCH] without an exit barrier. The strength of the C-H bond in butatriene is calculated to be 95.2 kcal mol^{-1}, so the H_2CCCCH + H products are 37.3 kcal mol^{-1} exothermic as compared to the initial reactants. The second dissociation channel of **et-s2** is elimination of molecular hydrogen with formation of the H_2CCCC molecule, butatriene carbene, overcoming a barrier of 88.9 kcal mol^{-1}. The H_2CCCC + H_2 products are about 20 kcal mol^{-1} more exothermic than i-C_4H_3 + H. The barrier for the H_2 elimination is 6.3 kcal mol^{-1} lower than the 'activation energy' required for the H loss from **et-s2** (since no distinct exit barrier exists for the H elimination, this activation energy coincides with the reaction endothermicity). But, on the other hand, the transition state for the H_2 loss is much tighter than loose variational transition states for the H elimination. The third possible decomposition channel of butatriene is dissociation to two vinylidene molecules through a cleavage of the central C=C bond. This reaction pathway is highly endothermic as the CCH_2 + CCH_2 products lie only 15.7 kcal mol^{-1} below the initial reactants and 116.8 kcal mol^{-1} above **et-s2**. The dissociation of butatriene to two CCH_2 molecules takes place without an exit barrier.

In addition to the dissociation channels considered above, **et-s2** can also rearrange to the cyclic methylenecyclopropene molecule **et-s5** by two different two-step pathways. The **et-s2** → **et-s5** isomerization requires three-member ring closure and a 1,2-shift of one of the hydrogen atoms. These two processes can occur in different order and hence two distinct rearrangement mechanisms were found. Along the **et-s2** → **et-s3** → **et-s5** pathway, the first step is a hydrogen atom 1,2-migration, which leads to the allenylcarbene intermediate **et-s3** ($HCCHCCH_2$). The calculated barrier for the H migration is 72.8 kcal mol^{-1}, and the resulting isomer **et-s3** lies 60.6 kcal mol^{-1} higher in energy than butatriene, but 71.9 kcal mol^{-1} below the $C_2(^1\Sigma_g^+)$ + C_2H_4 reactants. **et-s3** is

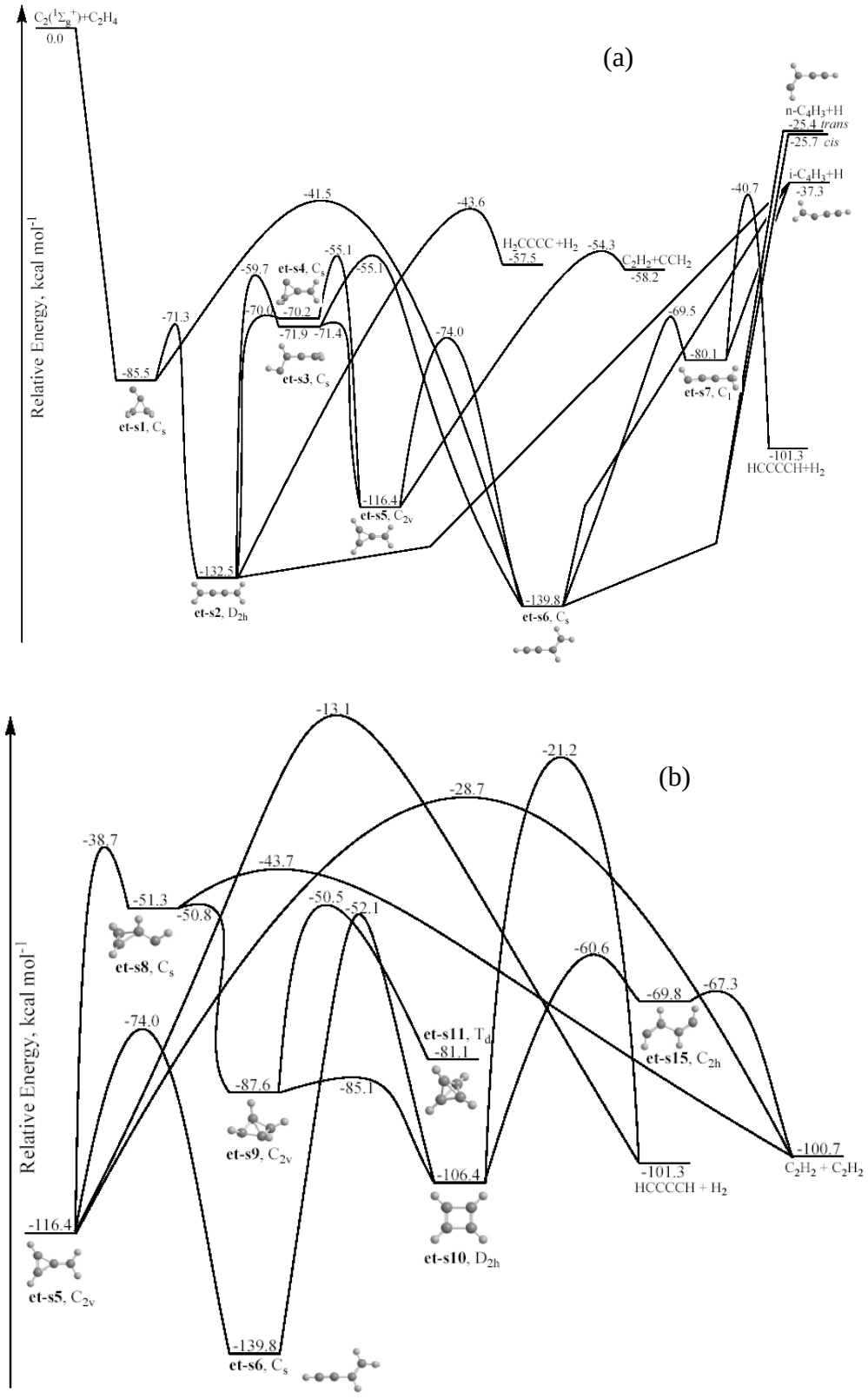

Figure 3. Potential energy diagram of the $C_2(^1\Sigma_g^+) + C_2H_4(^1A_g)$ reaction.

only a metastable intermediate, which easily undergoes ring closure to **et-s5** overcoming a tiny 0.5 kcal mol^{-1} barrier. The structure of $HCCHCCH_2$ is C_s-symmetric but non-planar, with CH_2 group perpendicular to the reflection plane and two CH groups in *cis* position with respect to each other. The $HCCHCCH_2$ structure with *trans* arrangement of the two CH groups is not a local minimum.

The calculations show that the metastable $HCCHCCH_2$ intermediate **et-s3** does not contribute to the H elimination channels. Allenylcarbene can decompose to propargyl $C_3H_3(X^2B_1)$ + $CH(X^2\Pi)$ by a cleavage of the terminal HC-CH bond. However, this product channel is calculated to be 16.3 kcal mol^{-1} endothermic and is not likely to be competitive even when it is energetically accessible.

Along the second possible pathway from **et-s2** to **et-s5** the ring closure occurs at the first step and is followed by the 1,2-H shift between two ring carbon atoms. The barrier for the ring closure is calculated to be 62.5 kcal mol^{-1} relative to **et-s2** and the cyclic intermediate **et-s4** formed after this rearrangement is only a metastable local minimum because the reverse ring-opening barrier from **et-s4** to **et-s2** is only 0.2 kcal mol^{-1}. In the forward direction, the 1,2-H shift in **et-s4** leads to the structure **et-s5** via a barrier of 15.1 kcal mol^{-1}. A comparison of two pathways from **et-s2** to **et-s5** shows that **et-s2** $\rightarrow$ **et-s3** $\rightarrow$ **et-s5** is energetically more favorable than **et-s2** $\rightarrow$ **et-s4** $\rightarrow$ **et-s5** because the highest barrier on the former (72.8 kcal mol^{-1} relative to **et-s2**) is 4.6 kcal mol^{-1} higher than that on the latter, 77.4 kcal mol^{-1}. In both cases, the 1,2-H shift is the rate-determining step.

The methylenecyclopropene intermediate **et-s5** residing 116.4 kcal mol^{-1} below $C_2(^1\Sigma_g^+)$ + C_2H_4 can dissociate into a number of different products. First, a cleavage of two single C-C bonds in the C_3 ring can result in the formation of acetylene + vinylidene over a barrier of 62.1 kcal mol^{-1}. The C_2H_2 + CCH_2 products reside 58.2 kcal mol^{-1} lower in energy than the initial reactants, so the **et-s5** $\rightarrow$ C_2H_2 + CCH_2 dissociation is 58.2 kcal mol^{-1} endothermic. Alternatively, methylenecyclopropene can dissociate directly to two acetylene molecules with a barrier of 87.7 kcal mol^{-1}. The C_2H_2 + C_2H_2 products of the initial $C_2(^1\Sigma_g^+)$ + C_2H_4 reaction are very exothermic as they lie 100.7 kcal mol^{-1} below the reactants. The other highly exothermic products of the $C_2(^1\Sigma_g^+)$ + C_2H_4 reaction are HCCCCH (diacetylene) + H_2 residing 101.3 kcal mol^{-1} lower in energy than the reactants. The HCCCCH + H_2 product pair can be formed from **et-s5** by 1,3-H_2 elimination overcoming a high barrier of 103.3 kcal mol^{-1}. Finally, **et-s5** can decompose to cyclopropenylidene c-$C_3H_2(X^1A_1)$ + methylene. The formation of the ground $CH_2(X^3B_1)$ is spin-forbidden and the products lie 1.5 kcal mol^{-1} higher in energy than $C_2(^1\Sigma_g^+)$ + C_2H_4. The formation of electronically excited $CH_2(^1A_1)$ is spin-allowed but energetically

is even less favorable. Therefore, we do not expect c-C_3H_2 + CH_2 to be significant reaction products.

The intermediate **et-s5** can alternatively be subjected to further isomerization. The most favorable channel is rearrangement to vinylacetylene **et-s6** via two different pathways. The first one involves 1,2-H shift to the central carbon accompanied with a rupture of the C-C bond bridged by the migrating hydrogen atom with a barrier of 42.4 kcal mol^{-1}. The second pathway occurs by a 1,4-H shift from the CH_2 at one end of the molecule to the CH group at the other end accompanied with the ring closure. However, the calculated barrier for the 1,4-H shift is 36.2 kcal mol^{-1} higher than that for the 1,2-H shift and so the 1,4-H migration pathway is not expected to be competitive. Isomer **et-s6** can also be formed directly from **et-s3** by a 2,3-hydrogen migration with a relatively low barrier of 16.8 kcal mol^{-1} with respect to **et-s3**.

Vinylacetylene **et-s6** is the most stable isomer of the C_4H_4 molecule and lies 139.8 kcal mol^{-1} lower in energy than the initial reactants. Dissociation of **et-s6** can occur by eliminations of hydrogen atoms from different positions or by a cleavage of the single C-C bond. The weakest C-H bond in vinylacetylene is at the carbon at position 3 (from left to right in Figure 3). Its cleavage is endothermic by 102.5 kcal mol^{-1}, occurs without an exit barrier, and leads to the H_2CCCCH (i-C_4H_3) + H products with overall reaction energy of –37.3 kcal mol^{-1}. On the other hand, hydrogen loss from the terminal CH_2 group results in *cis* (*E*) and *trans* (*Z*) conformations of the n-C_4H_3 radical, which lie 11.6 and 11.9 kcal mol^{-1} higher in energy than i-C_4H_3, respectively. A rupture of the ordinary C-C bond in **et-s6** leads to the C_2H_3 + C_2H products. This C-C bond is stronger than the C-H bonds and the dissociation is 138.6 kcal mol^{-1} endothermic. The vinyl + ethynyl products lie only 1.2 kcal mol^{-1} below the initial reactants and should not significantly contribute to the $C_2(^1\Sigma_g^+)$ + C_2H_4 reaction. Another theoretical possibility for the formation of the C_2H_3 + C_2H products is a direct hydrogen abstraction from ethylene by singlet dicarbon. However, we were not able to locate a first-order saddle point for this process. The ground state singlet potential energy surface is strongly attractive when $C_2(^1\Sigma_g^+)$ approaches the double bond in ethylene and adds to it without a barrier. Therefore, we do not anticipate the H-abstraction to play an important role unless some direct trajectories exist that are accessible at high collision energies.

Isomer **et-s6** can undergo further isomerization. It can rearrange to methylpropargylene $HCCCCH_3$ **et-s7** by 3,4-H migration over a barrier of 70.3 kcal mol^{-1}. Alternatively, cyclobutadiene **et-s10** can be formed overcoming a higher barrier of 87.7 kcal mol^{-1}. In the reverse direction, the isomerization process can be described as a 1,2-H shift in cyclobutadiene, which takes place synchronously with a cleavage of the single C-C bond between the carbon

atoms involved in the hydrogen migration. Formally, the vinylvinylidene structure is produced from **et-s10** as a result of this rearrangement, but vinylvinylidene is, at best, a metastable local minimum, which easily isomerizes to the much more favorable vinylacetylene intermediate **et-s6** by the 2,1-H shift. There exist two possible dissociation pathways of methylpropargylene **et-s7**, which resides 80.1 kcal mol^{-1} lower in energy than $C_2(^1\Sigma_g^+)$ + C_2H_4. The H loss from the CH_3 group leads to i-C_4H_3 + H without an exit barrier. The C-H bond strength in the methyl group of **et-s7** is calculated to be rather low, only 42.8 kcal mol^{-1}. Theoretically, the hydrogen atom can also be eliminated from the terminal CH group. However, our earlier calculations [47] have shown that the $CCCCH_3$ isomer of C_4H_3 is 39.5 kcal mol^{-1} less favorable than H_2CCCCH and hence the C-H bond in CH is much stronger than that in CH_3 and the cleavage of the former is not likely to compete with the cleavage of the latter. If the C-CH_3 carbon-carbon bond in **et-s7** is broken, the reaction products are l-C_3H + CH_3. However, these products reside only 1.9 kcal mol^{-1} below the initial reactants and the C-C bond is 35.4 kcal mol^{-1} stronger than the C-H bond in the methyl group. Consequently, we do not expect the l-C_3H + CH_3 products to play a significant role in the reaction.

The cyclobutadiene isomer **et-s10**, 106.4 kcal mol^{-1} lower in energy than $C_2(^1\Sigma_g^+)$ + C_2H_4, can be formed not only from methyacetylene **et-s6**, but also from **et-s5** through a three-step pathway involving intermediates **et-s8** and **et-s9**. At the first step of this pathway, the molecule undergoes hydrogen atom migration from the CH_2 group in **et-s5** to the central carbon to form a non-planar C_s-symmetric three-member ring structure **et-s8**, 51.3 kcal mol^{-1} below the initial reactants, over a barrier of 77.7 kcal mol^{-1}. **et-s8** is a metastable intermediate, which is subjected to a closure of the second three-member cycle to produce another bicyclic C_{2v}-symmetric intermediate **et-s9**, 87.6 kcal mol^{-1} below $C_2(^1\Sigma_g^+)$ + C_2H_4. The barrier separating **et-s8** from **et-s9** is only 0.5 kcal mol^{-1}. Structure **et-s9** is also a metastable local minimum and a cleavage of the weak diagonal C-C bond adjoining the two three-member rings leads to cyclobutadiene **et-s10** via a 2.5 kcal mol^{-1} barrier. Meanwhile, **et-s9** also serves as a precursor for the formation of tetrahedrane **et-s11**. The formation of an additional C-C bond between two unconnected carbon atoms in **et-s9** results in the tetrahedral structure overcoming a barrier of 37.1 kcal mol^{-1}. Thus, the tetrahedrane isomer of C_4H_4 can be formed either from methylenecyclopropene via the **et-s5** $\rightarrow$ **et-s8** $\rightarrow$ **et-s9**$\rightarrow$ **et-s11** pathway with the highest barrier of 77.7 kcal mol^{-1} relative to **et-s5**, or from vinylacetylene or cyclobutadiene via the **et-s6** $\rightarrow$ **et-s10** $\rightarrow$ **et-s9**$\rightarrow$ **et-s11** pathway with the highest barriers of 89.3 and 55.9 kcal mol^{-1} relative to **et-s6** and **et-s10**, respectively, corresponding to the last reaction step. Tetrahedrane resides in a potential well of 81.1 kcal mol^{-1} and is separated from **et-s9** by a barrier of 30.6 kcal mol^{-1}.

Among the two reaction mechanisms leading from **et-s5** to cyclobutadiene **et-s10**, **et-s5** → **et-s6**→ **et-s10** and **et-s5** → **et-s8** → **et-s9** → **et-s10**, the former is preferable because the highest in energy transition state for this pathway is 13.4 kcal mol^{-1} lower than the critical transition state on the latter pathway. For the same reason, the formation of tetrahedrane is more likely via **et-s6**, **et-s10**, and **et-s9** than via **et-s8** and **et-s9.** Cyclobutadiene can decompose directly to diacetylene + H_2 by 1,2-H_2 elimination accompanied with the four-member ring opening. However, such decomposition is unlikely because the barrier is high, 85.2 and 80.1 kcal mol^{-1} in the forward and reverse directions, respectively.

Cyclobutadiene can be also formed directly from allenylcarbene **et-s3** by a 4,3-H shift. Formally, this hydrogen migration should lead to a *cis*-$HC^{\cdot}$=CH=CH=$CH^{\cdot}$ structure and the corresponding local minimum was indeed found at the spin-unrestricted UB3LYP level of theory. However, this structure features two unpaired electrons with opposite spins located at different molecular orbitals. Such open-shell singlet wave functions may not be properly described by single reference methods and therefore CASSCF(12,12) geometry optimization was carried out. This optimization converged to cyclobutadiene **et-s10** allowing us to conclude that *cis*-$HC^{\cdot}$=CH=CH=$CH^{\cdot}$ is not a local minimum and allenylcarbene is connected directly with cyclobutadiene. The barrier for this rearrangement is very high, 53.3 kcal mol^{-1} relative to **et-s3** and it is not likely to occur considering that **et-s3** is a metastable intermediate separated from **et-s5** by a barrier as low as 0.5 kcal mol^{-1}.

A *trans* conformation of the $HC^{\cdot}$=CH=CH=$CH^{\cdot}$ structure corresponds to a local minimum **et-s15** and is involved in the two-step dissociation pathway of cyclobutadiene to two acetylene molecules. Because of a multireference character of wave functions for **15** and the adjoining transition states, their energies were computed at the CASPT2/6-311+G(3df,2p)//CASSCF/6-311G(d,p) level. Similar multireference calculations were also carried out for cyclobutadiene to obtain relative CASPT2 energies of **et-s15** and the two transition states with respect to **et-s10**. On the pathway from **et-s10** to **et-s15**, the ring opening is followed by rotation around the central C-C bond. As soon the rotation is completed, the *cis* conformation undergoes a spontaneous ring closure. The barrier for the ring opening/rotation in **et-s10** is calculated to be 45.8 kcal mol^{-1}. **et-s15** decomposes to C_2H_2 + C_2H_2 by cleaving the central C-C bond via a low 2.5 kcal mol^{-1} barrier. The overall dissociation mechanism can be written as cyclobutadine **et-s10** → **et-s15** → C_2H_2 + C_2H_2 with the highest barrier at the first step.

We also tried to find a transition state for direct dissociation of tetrahedrane to two acetylene molecules. However, the optimization converged to a transition state connecting C_2H_2 + C_2H_2 with the cyclic isomer **et-s8**. Thus,

the pathway from tetrahedrane to two acetylenes involves sequential cleavage of four C-C bonds via three steps: **et-s11** → **et-s9** (one bond is broken), **et-s9** → **et-s8** (another bond is cleaved), and finally **et-s8** → C_2H_2 + C_2H_2 (two C-C bonds are broken in an asynchronous manner). The highest barrier, 37.4 kcal mol^{-1} relative to **et-s11**, is found for the last reaction step. Considering the reverse C_2H_2 + C_2H_2 reaction, we conclude that it can lead to cyclobutadiene (C_2H_2 + C_2H_2 → **et-s15** → **et-s10** with the critical barrier of 40.1 kcal mol^{-1} with respect to two acetylenes) and to tetrahedrane (C_2H_2 + C_2H_2 → **et-s8** → **et-s9** → **et-s11**, 57.0 kcal mol^{-1}). However, the formation of tetrahedrane through the latter pathway is very unlikely because intermediate **et-s9** would isomerize to cyclobutadiene **et-s10** rather than to **et-s11** over a low 2.6 kcal mol^{-1} barrier. The pathway from C_2H_2 + C_2H_2 to methylenecyclopropene **et-s5** exhibits even higher barrier of 72.0 kcal mol^{-1}.

4.2. Product branching ratios of the $C_2(^1\Sigma_g^+)$ + $C_2H_4(^1A_g)$ reaction

According to the calculated energies of intermediates and transition states, the most favorable product channels of the $C_2(^1\Sigma_g^+)$ + C_2H_4 reaction are acetylene + vinylidene, **et-s1** → **et-s2** → **et-s3** → **et-s5** → C_2H_2 + CCH_2, with the highest in energy transition state lying 54.1 kcal mol^{-1} below the initial reactants, followed by **et-s1** → **et-s2** → $H_2C{=}C{=}C{=}C$: + H_2 (TS for the H_2 loss, -43.6 kcal mol^{-1} relative to $C_2(^1\Sigma_g^+)$ + C_2H_4), and **et-s1** → **et-s2** → $H_2C{=}C{=}C{=}CH^{\cdot}$ + H, where the highest in energy stationary structure corresponds to the products, -37.3 kcal mol^{-1} relative to the reactants. However, this consideration does not take into account densities of states of the transition states involved, i.e., their looseness or tightness.

In order to quantify relative yields of various possible products, we carried out microcanonical RRKM calculations of energy-dependent rate constants for individual reaction steps and solved kinetic equations. It should be noted that this treatment assumes a complete energy randomization, which is not necessarily the case for reactive intermediates formed in the $C_2(^1\Sigma_g^+)$ + C_2H_4 reaction. Also, our treatment cannot account for impact-parameter dependent reaction dynamics. Therefore, the product branching ratios calculated here might differ from those derived in actual crossed beam experiments. The internal energy available to intermediates and transition states was taken as the energy of chemical activation, i.e., the relative energy with respect to the C_2 $(^1\Sigma_g^+)$ + C_2H_4 reactants plus collision energy, E_{col}, assuming that the dominant fraction of the latter is converted to the vibrational energy and only a small portion goes to their rotational excitation. This assumption is most valid for reactive collisions with a small impact parameter, which do not introduce a significant torque.

The calculated product branching ratios of the $C_2(^1\Sigma_g^+)$ + C_2H_4 reaction for E_{col} = 0-10 kcal mol^{-1} are collected in Table 1.

Table 1. Calculated branching ratios (%) of the $C_2(^1\Sigma_g^+)$ + C_2H_4 and $C(^1D)$ + C_3H_4 reactions at different collision energies.

	E_{col}, kcal mol^{-1}										
Products	0	1	2	3	4	5	6	7	8	9	10
CCH_2 + CCH_2	0.09	0.11	0.13	0.15	0.18	0.20	0.23	0.27	0.30	0.34	0.37
C_2H_2 + CCH_2	48.63	47.04	45.48	44.03	42.70	41.42	40.12	38.89	37.71	35.93	35.46
C_2H_2 + C_2H_2	1.83	1.78	1.73	1.69	1.65	1.61	1.57	1.54	1.51	1.45	1.45
HCCCCH + H_2	1.75	1.76	1.77	1.78	1.76	1.78	1.79	1.78	1.78	1.74	1.75
C_2H_3 + C_2H	0	0	0	0	0	0	0	0	0	0	0
H_2CCCC + H_2	6.06	6.22	6.36	6.53	6.72	6.85	7.00	7.15	7.29	7.58	7.57
H_2CCCCH + H	41.25	42.67	44.05	45.30	46.45	47.55	48.65	49.69	50.70	52.21	52.59
from **et-s2**	30.56	31.75	32.88	33.90	34.96	35.81	36.74	37.66	38.54	40.19	40.29
from **et-s6**	5.06	5.11	5.16	5.22	5.25	5.27	5.30	5.31	5.33	5.23	5.32
from **et-s7**	5.63	5.81	6.01	6.18	6.24	6.47	6.61	6.72	6.83	6.79	6.98
c-HCCHCCH + H	0.22	0.24	0.26	0.28	0.30	0.33	0.35	0.37	0.40	0.41	0.44
t-HCCHCCH + H	0.18	0.20	0.21	0.23	0.25	0.27	0.29	0.31	0.33	0.34	0.37

One can see that two reaction channels are most important. At E_{col} = 0, the branching ratios of the C_2H_2 + CCH_2 and $H_2C{=}C{=}C{=}CH^{\cdot}$ (i-C_4H_3) + H products are 48.6% and 41.3%, respectively. The third significant reaction channel, 6.1%, is H_2CCCC + H_2. Minor product channels include diacetylene + H_2 (1.8%), *E* (*cis*) and *Z* (*trans*) conformations of n-C_4H_3 + H (totally, 0.4%), and acetylene + acetylene (under 1.8%). As the collision energy increases to 10 kcal mol^{-1}, the relative yield of i-C_4H_3 increases to 52.6%, but that of C_2H_2 + CCH_2 decreases to 35.5%. The branching ratios of the other products are affected only slightly; the most significant change found among them is an increase of the $H_2C{=}C{=}C{=}C{:}$ + H_2 branching ratio by 1.5%. Calculations of relative yields of i-C_4H_3 + H show that about 3/4 of these products are formed from butatriene **et-s2**, and 1/8 each from vinylacetylene **et-s6** and methylpropargylene **et-s7**.

4.3. $C_2(^3\Pi_u)$ + $C_2H_4(^1A_g)$: Triplet potential energy surface and product yields

The initial addition of $C_2(^3\Pi_u)$ to the π-system of ethylene on the triplet surface (Figure 4) most likely occurs without activation, as our geometry optimization of the $C_2(^3\Pi_u)$ + C_2H_4 addition transition state at the B3LYP/6-311G** and QCISD/6-311G** levels do not give any barrier [52,53], which agrees with the earlier lower level HF/3-21G calculations [24]. We did obtain a barrier of 3.7 kcal mol^{-1} at the G2M(RCC,MP2) level with the MP2/6-311G** optimized transition state geometry, but this result is probably less reliable than

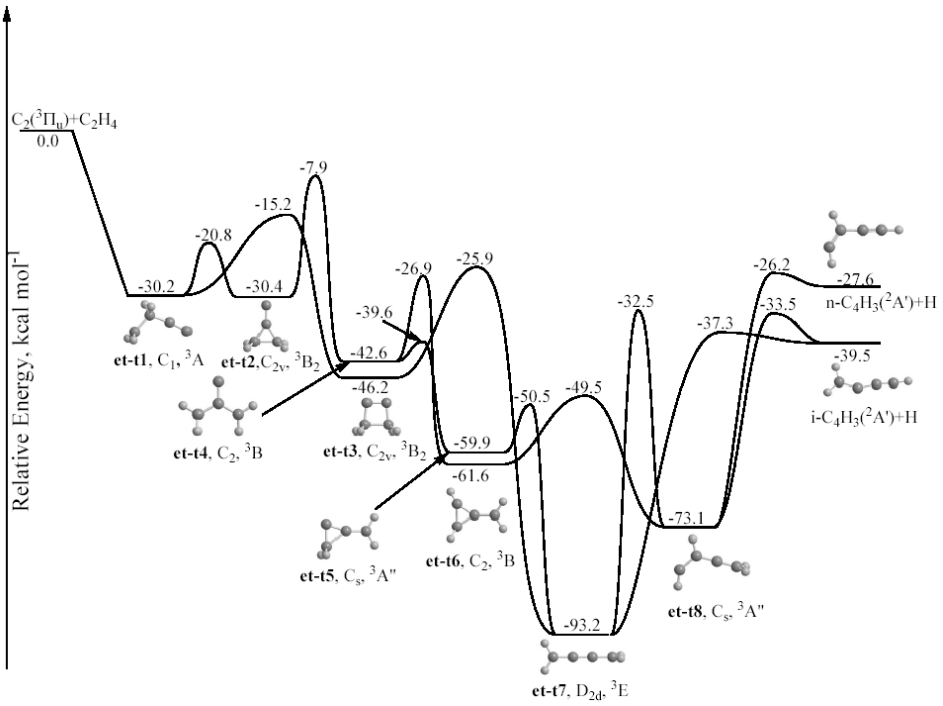

Figure 4. Potential energy diagram of the $C_2(^3\Pi_u) + C_2H_4(^1A_g)$ reaction.

those of the B3LYP and QCISD calculations, because kinetic measurements [18] showed that the activation barrier is lower than 1 kcal mol^{-1}, if exists at all.

The C_2 addition forms a chain intermediate **et-t1** bound by 30.2 kcal mol^{-1} with respect to the reactants. This intermediate can undergo a ring closure forming a three-member ring intermediate **et-t2** with a barrier of 9.4 kcal mol^{-1}, which in turn would rearrange to a branch isomer **et-t4** over a 22.5 kcal mol^{-1} barrier, then to another three-member cyclic intermediate **et-t5** (the barrier is 15.7 kcal mol^{-1}), which ring-opens to linear triplet butatriene **et-t7** residing 93.2 kcal mol^{-1} below the reactants (the barrier is 9.4 kcal mol^{-1}). **et-t7** loses a hydrogen atom to produce i-C_4H_3 with the overall reaction exothermicity of 39.5 kcal mol^{-1} over an exit barrier of 2.2 kcal mol^{-1} relative to the products. The highest barrier on this pathway is located between **et-t2** and **et-t4** with the corresponding transition state lying 7.9 kcal mol^{-1} below the reactants. A second route from **et-t1** to **et-t7** involves the four-member ring isomer **et-t3**, triplet cyclobutyne. The ring closure from **et-t1** to **et-t3** is characterized by a barrier of 15.0 kcal mol^{-1} and the corresponding transition state is 15.2 kcal mol^{-1} lower in energy than the reactants. Then, **et-t3** undergoes ring opening along the CH_2-CH_2 bond to yield **et-t7** with a barrier of 20.3 kcal mol^{-1}. The triplet cyclobutyne corresponds to a well-defined local minimum at 46.2 kcal mol^{-1} below the reactants and is stabilized by a barrier of ~20 kcal mol^{-1} with respect to the ring opening. The ground state of cyclobutyne on the triplet PES

is $^3B_2$; the molecule can be described in terms of three single C-C bonds and one C=C double bond in the four-member ring. The two unpaired electrons are localized on the hydrogen-free carbon atoms. Both pathways leading from **et-t1** to **et-t7** are expected to compete.

An alternative reaction pathway leading to both i- and n-C_4H_3 isomers also exists. The branched intermediate **et-t4** can undergo a three-member ring closure accompanied with a 1,3-H migration to produce the triplet methylenecyclopropene intermediate **et-t6** (61.6 kcal mol^{-1} below the reactants) with a barrier of 15.7 kcal mol^{-1}. Next, **et-t6** can ring-open to the triplet allenylcarbene isomer **et-t8** overcoming a barrier of 12.1 kcal mol^{-1}. The latter can be also obtained from triplet butatriene **et-t7** by a 1,2-H shift, but in this case the barrier is much higher, 60.7 kcal mol^{-1}. **et-t8** residing 73.1 kcal mol^{-1} lower in energy than the $C_2(^3\Pi_u)$ + $C_2H_4(^1A_g)$ reactants can decompose to i-C_4H_3 by eliminating the hydrogen atom from the non-terminal CH group (via a barrier of 39.6 kcal mol^{-1}) or to n-C_4H_3 by cleaving a C-H bond in the CH_2 group (via a barrier of 46.9 kcal mol^{-1}).

In order to quantify the role of the two pathways leading from **et-t1** to the triplet butatriene, we carried out RRKM calculations of the triplet reaction rate constants. The rates for individual steps computed for the collision energy of 6.9 kcal mol^{-1} were then employed to solve kinetic equations for the steady-state regime and to calculate the branching ratio of the **et-t1** → **et-t3** → **et-t7** pathway vs. **et-t1** → **et-t2** → **et-t4** → **et-t5** → **et-t7** pathway. The results show that about 90% of triplet butatriene are formed via the path involving the triplet cyclobutyne intermediate **et-t3** and only 10% are produced by the multistep mechanism via the three-member ring intermediates. The branching ratios were found to be not sensitive to the collision energy; for instance, at zero collision energy they change by less than 1%. Thus, the elusive cyclobutyne in the triplet electronic state is a key intermediate of the $C_2(^3\Pi_u)$ + C_2H_4 reaction. From the rate constants, we can estimate that the lifetime of triplet cyclobutyne under single collision conditions is about 3 ps, while that of triplet butatriene **et-t7** is about 4 ps, hence both intermediates are expected to be observable spectroscopically. Since ~10% of reaction trajectories can proceed via the **et-t4** intermediate, we have also considered the possibility of the formation of isomer **et-t6**, which can be a precursor of n-C_4H_3. From **et-t4**, the reaction can go to either **et-t5** overcoming a low barrier of 3.0 kcal mol^{-1} or to **et-t6** via a significantly higher barrier of 15.7 kcal mol^{-1}. Then, **et-t5** readily rearranges to triplet butatriene **et-t7**, whereas **et-t6** rapidly isomerizes to triplet allenylcarbene **et-t8**. A comparison of RRKM rate constants for the **et-t4** → **et-t5** and **et-t4** → **et-t6** steps calculated for collision energies between 0 and 10 kcal mol^{-1} shows that the former reaction is much faster than the latter, by the factors varying from 38.3 to 20.2 as the collision energy increases. Thus, even at E_{col} = 10 kcal mol^{-1}, the probability to form **et-t8** from **et-t4** does not exceed

5%. Since the probability that the reaction will pass through the **et-t4** intermediate is in the range of 10%, the formation of **et-t8** is unlikely, less than 0.5%. Note that the production of **et-t8** from **et-t7** is also improbable, as the rate constant for H elimination from triplet butatriene to produce i-C_4H_3 is a factor of 40-35 higher than that for the 1,2-H shift to **et-t8** at E_{col} = 0-10 kcal mol^{-1}. If a small amount of **et-t8** is produced, it can decompose to i-C_4H_3 and n-C_4H_3 with nearly equal probabilities. Although the barrier for the H-loss from the CH_2 group to form n-C_4H_3 is 7.3 kcal mol^{-1} higher than that to produce i-C_4H_3, the former process has a looser transition state and higher reaction path degeneracy (2). As a result, the calculated **et-t8** $\rightarrow$ i-C_4H_3 + H and **et-t8** $\rightarrow$ n-C_4H_3 + H rate constants are similar; their ratio varies from 1.56 to 0.98 as the collision energy increases from 0 to 10 kcal mol^{-1}. In summary, we can conclude that for the $C_2(^3\Pi_u)$ + C_2H_4 reaction, i-C_4H_3 is the major product, formed mostly via the decomposing triplet butatriene complex through an exit barrier of 2.2 kcal mol^{-1}; only trace amounts of n-C_4H_3 may be produced at high collision energies. Spin-allowed decomposition of triplet C_4H_4 to any other products is highly unfavorable as compared to i-C_4H_3 + H. For instance, $C_2H_2(^1\Sigma_g^+)$ + $C_2H_2(^3B_2)$, $C_2H_2(^1\Sigma_g^+)$ + $H_2CC(^3B_2)$, CH_3 + c-C_3H, CH_3 + l-C_3H, and $CH_2(^3B_1)$ + c-C_3H_2 are calculated to be less exothermic than i-C_4H_3 + H by 26.6, 29.9, 33.3, 35.7, and 39.1 kcal mol^{-1}, respectively, and therefore are not likely to be observable in the $C_2(^3\Pi_u)$ + C_2H_4 reaction.

4.4. Comparison with experimental results

The chemical dynamics of the formation of the i-$C_4H_3(X^2A')$ radical together with its partially deuterated isotopomers were investigated in recent crossed molecular beams experiments of dicarbon molecules in the $X^1\Sigma_g^+$ and $a^3\Pi_u$ electronic states with (partially deuterated) ethylene at several collision energies between 2.9 and 9.8 kcal mol^{-1} [53,54]. The center-of-mass angular distributions suggested that the reaction dynamics on the singlet and triplet surfaces are indirect and involve butatriene reaction intermediates. In case of the C_2/C_2H_4 reaction, the 'symmetric' singlet butatriene intermediate would lead solely to a symmetric center-of-mass angular distribution; however, in combination with isotopically labeled reactants, as was deduced from the experimental data, triplet butatriene intermediates excited to B/C like rotations likely account for the observed asymmetries in the center-of-mass angular distributions at higher collision energies. These findings agree with the results of our ab initio/RKKM calculations that most of the i-C_4H_3 products are formed from the singlet **et-s2** and triplet **et-t7** butatriene intermediates. The translational energy distributions were also indicative of the involvement of both the triplet and singlet surfaces which lead both to the i-$C_4H_3(X^2A')$ radicals through lose (singlet) and tight (triplet) exit transitions states; note that

no exit barrier was found for the H loss from **et-s2** on the singlet surface, whereas on the triplet PES the exit barrier for H elimination from **et-t2** is low, 2.2 kcal mol^{-1}. Also, the experiments helped to determine the enthalpy of formation of the i-$C_4H_3(X^2A')$ radical to be about 120.5 ± 2.4 kcal mol^{-1} in good agreement with the computational studies suggesting ~119 kcal mol^{-1}. The explicit identification of the resonance-stabilized i-$C_4H_3(X^2A')$ radical proposes that the reaction of dicarbon with ethylene can lead to formation of i-$C_4H_3(X^2A')$ in combustion flames; the n-$C_4H_3(X^2A')$ isomer was not observed in this reaction, which is also in agreement with our computational results. This conclusion also correlates with Hansen's et al. flame experiments at the Advanced Light Source observing only the i-C_4H_3 (X^2A') radical in hydrocarbon flames [55].

The experimental data also showed that the product angular distributions in the $C_2/C_2H_2D_2$ systems are less asymmetric as compared to the C_2/C_2H_4 reaction. This is apparently an effect of the substitution of two hydrogen atoms by two deuterium atoms and the inherent reduction of the frequency of the C-D bending and stretching modes compared to C-H, which should result in an enhanced life time of the intermediates. Our statistical computations confirm this; we found longer life times with respect to H and D loss for the singlet and triplet D2-butatriene intermediates (304-311 and 5.9 ps, respectively) as compared to 180 and 3.7 ps, respectively, in the case of singlet and triplet butatriene. This trend is amplified in the C_2/C_2D_4 system, which shows a forward-backward symmetric center-of-mass angular distribution. Here, we found life times of the singlet and triplet D4-butatriene of 542 and 10.5 ps, respectively. Again, these life times are longer than the corresponding singlet and triplet butatriene intermediates at a similar collision energy.

Unfortunately, C_2H_2 heavy fragments, which, in the case of statistical behavior, should constitute up to ~49% of the total products in the $C_2(^1\Sigma_g^+)$ + C_2H_4 reaction at low collision energies, were difficult to detect in the molecular beams experiments; the detector is currently switched to soft electron impact ionization mode to investigate this hitherto elusive channel. On the other hand, in the matrix isolation experiment on photodissociation of allenylcarbene, only vinylacetylene and acetylene were detected [56]. In this experiment, the C_4H_4 intermediates could be stabilized by secondary collisions and therefore the observation of vinylacetylene, the most stable C_4H_4 isomer, is not surprising. Vinylidene is a metastable isomer of C_2H_2, which apparently did not survive isomerization to acetylene. Non-observation of i-C_4H_3 in the matrix isolation experiment indicates that this product is unstable with respect to secondary encounters (such as recombination with H atoms).

The C_2H_2 products could not be observed in the recent experimental work by Stearns et al. [57] who investigated photodissociation of vinylacetylene **et-s6** at 220 nm and detected only C_4H_3 and C_4H_2 primary products with

branching ratios of 3-10:1. However, the authors speculated acetylene to be the major reaction product and its non-observation was attributed to its high ionization potential, so that C_2H_2 molecules could not be detected by 118 nm photoionization. Theoretical simulations in this work which were performed for the low temperature and pressure corresponding to Titan's atmosphere and gave the relative product yields of C_2H_2:C_4H_2:C_4H_3 as 66:7:27, which is qualitative agreement with our results for collision-free conditions. In our calculations, the $C_2(^1\Sigma_g^+)$ + C_2H_4 reaction initially accesses another region of the C_4H_4 PES, the butatriene intermediate **et-s2**, which can eventually rearrange to vinylacetylene. The latter in this case possesses chemical activation energy of 139.8 kcal mol^{-1}, which is higher than 130 kcal mol^{-1} available when the photodissociation reaction is initiated by absorption of a 220 nm photon. This causes quantitative differences in the calculated product branching ratios. However, our results show a trend of the increasing relative yield of C_2H_2 with the decreasing available energy. C_2H_2 has been detected experimentally as a product of the C_4H_4 decomposition by Hidaka [58] in a shock tube study of the vinylacetylene pyrolysis at 1500 K. Hidaka estimated the C_2H_2:C_4H_2 branching ratio as 7-10:1 and did not observe C_4H_3, which apparently undergoes secondary dissociation under shock tube conditions. Stearns et al. [57] simulated the shock tube pressure and temperature conditions and calculated the C_2H_2:C_4H_2:C_4H_3 branching ratios to be 61:1:38.

5. Reactions of C_2 with methylacetylene

5.1. $C_2(^1\Sigma_g^+)$ + $CH_3CCH(^1A_1)$: Singlet potential energy surface

Schematic potential energy diagram for the reaction of singlet dicarbon with methylacetylene [59] is shown in Figure 5. When a singlet C_2 molecule adds to CH_3CCH, two different C_5H_4 isomers can be initially produced, a C_s-symmetric three-member ring intermediate **ma-s1**, formed by the addition of C_2 to the triple C≡C bond in an end-to-side manner and residing 70.9 kcal mol^{-1} below the reactants, and a four-member ring structure **ma-s2** produced by the side-to-side addition and lying 70.5 kcal mol^{-1} below the reactants. Both addition processes are calculated to be barrierless.

At the next reaction step, **ma-s2** can isomerize to the most stable singlet C_5H_4 intermediate **ma-s3**, C_{3v}-symmetric methyldiacetylene H_3C-C≡C-C≡C-H, residing 137.6 kcal mol^{-1} lower in energy with respect to $C_2(^1\Sigma_g^+)$ + CH_3CCH. Just like in the case of the **ac-s2** → **ac-s3** rearrangement in the C_2 + acetylene reaction, this process is rather complicated. The (CH_3)C-CH bond is not cleaved directly but instead one of the dicarbon atoms formally inserts between two acetylenic C atoms, and the second takes the terminal position in the carbon chain, which is followed by a spontaneous hydrogen shift to this terminal carbon. The barrier separating **ma-s2** and **ma-s3** is relatively low,

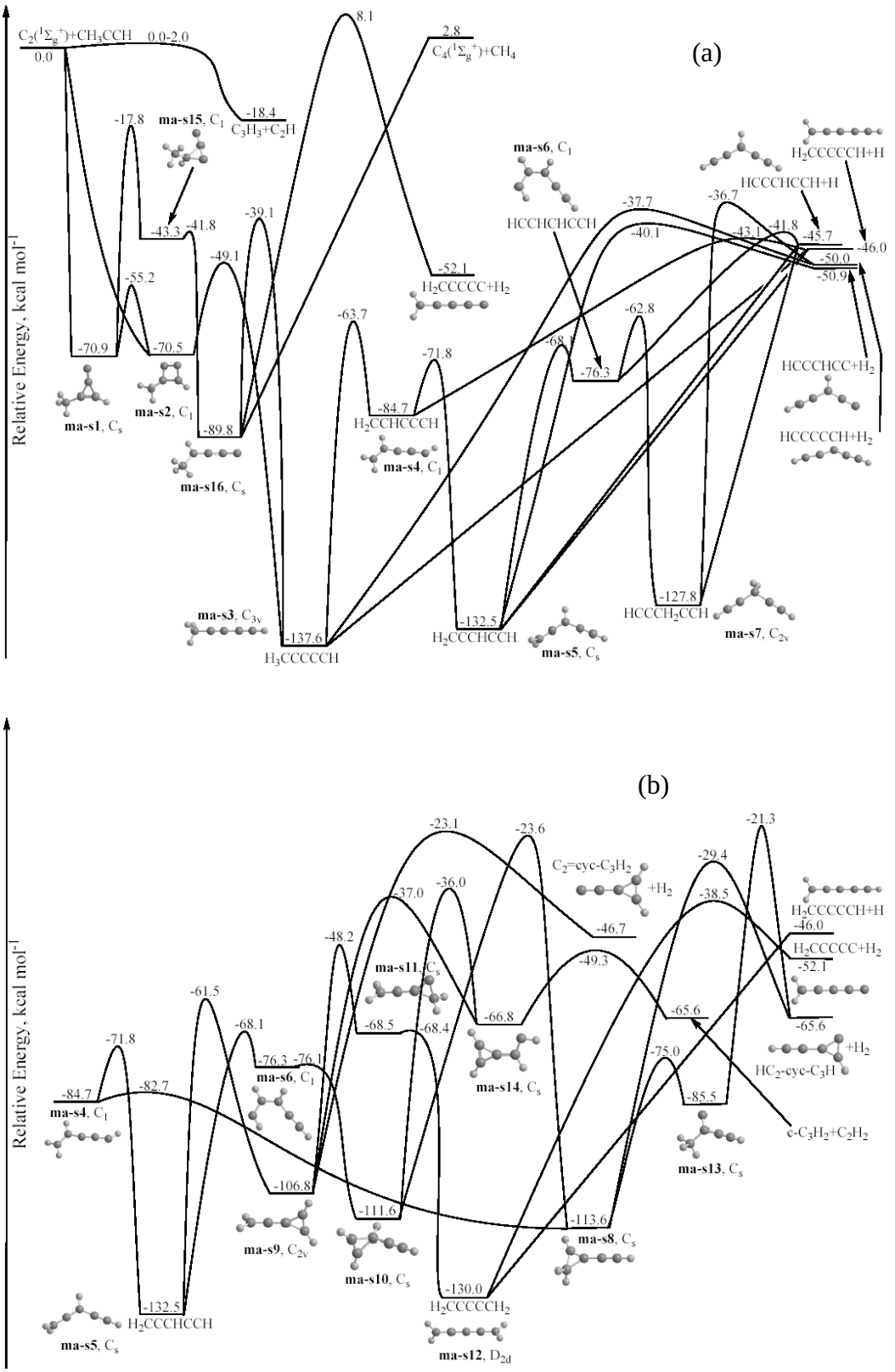

Figure 5. Potential energy diagram of the $C_2(^1\Sigma_g^+)$ + $CH_3CCH(^1A_1)$ reaction.

21.4 kcal mol^{-1}, as the respective transition state lies 49.1 kcal mol^{-1} below the reactants. Therefore, we can expect that methyldiacetylene **ma-s3** can be rapidly produced from the reactants if the initial intermediates **ma-s1** and **ma-s2** are not collisionally deactivated, for instance, in combustion flames and in high-density cometary comae. As seen in Figure 5, the fate of the methyldiacetylene isomer **ma-s3** can be threefold. First, it can lose a hydrogen atom from the CH_3 group and yield the i-C_5H_3 [$H_2CCCCCH$ (C_{2v},$^2B_1$)] + H products without an exit barrier. The H elimination is calculated to be 91.6 kcal mol^{-1} endothermic, however, the products reside 46.0 kcal mol^{-1} below the initial $C_2(^1\Sigma_g^+)$ + CH_3CCH reactants. A loss of the acetylenic hydrogen is much less favorable because the H_3CCCCC (C_s,$^2A''$) structure lies about 41 kcal mol^{-1} above $H_2CCCCCH$ [60]. Therefore, although the $C_2(^1\Sigma_g^+)$ + $CH_3CCH \rightarrow$ **ma-s3** $\rightarrow H_3CCCCC + H$ reaction would be slightly exothermic, it is unfavorable kinetically. The second possible dissociation channel of methyldiacetylene is H_2 elimination from the CH_3 group. This leads to the formation of the HCCCCCH (C_{2v}, $^1A_1$) molecule overcoming a barrier of 99.9 kcal mol^{-1}. The HCCCCCH (C_{2v}, $^1A_1$) + H_2 products reside 50.0 kcal mol^{-1} below $C_2(^1\Sigma_g^+)$ + CH_3CCH and 4.0 kcal mol^{-1} lower in energy than $H_2CCCCCH$ (C_{2v},$^2B_1$) + H. However, the exit barrier for the H_2 elimination from **ma-s3** is 8.3 kcal mol^{-1} higher than the energy required to split an atomic hydrogen from the CH_3 group. The third possibility is 1,2-migration of a CH_3 hydrogen to the neighboring C atom, which results in the non-symmetric intermediate $H_2CCHCCCH$ **ma-s4**. **ma-s4** is 52.9 kcal mol^{-1} less stable than **ma-s3** and the barrier for the H shift is calculated to be 73.9 kcal mol^{-1}.

Next, intermediate **ma-s4** can eliminate the hydrogen atom from the carbon in position 2; H losses from the other C atoms are unfavorable in terms of the product energies. The **ma-s4** $\rightarrow H_2CCCCCH + H$ reaction is 38.7 kcal mol^{-1} endothermic and exhibits an exit barrier of 2.9 kcal mol^{-1}, which can be attributed to two factors: the fact that in the reverse reaction the H atom adds to C_2 but the unpaired electron (the radical site) in $H_2CCCCCH$ is located on C_1, and a relatively low exothermicity of the recombination reaction. Alternatively to the H loss, **ma-s4** can undergo a second, 2,3-H shift to the central carbon C_3 over a barrier of 12.9 kcal mol^{-1}, and the migration results in much more stable intermediate **ma-s5**, $H_2CCCHCCH$.

The latter lies 132.5 kcal mol^{-1} below the reactants and is only 5.1 kcal mol^{-1} less stable than methyldiacetylene **ma-s3**. **ma-s5** can eliminate H atoms from C_3 and C_1 to produce the i-C_5H_3 ($H_2CCCCCH$) and n-C_5H_3 [$HCCCHCCH$ (C_{2v},$^2B_1$] isomers of the C_5H_3 radical, respectively, without exit barriers. The energy difference between the two products is only 0.3 kcal mol^{-1} and the two H eliminations from $H_2CCCHCCH$ are endothermic by 86.5 and 86.8 kcal mol^{-1}, respectively. Molecular hydrogen can also be split from the CH_2 group in **ma-s5** via a barrier of 92.4 kcal mol^{-1}. Then, the HCCCHCC (C_s)

isomer of C_5H_2 is formed with endothermicity of 81.6 kcal mol^{-1}; the HCCCHCC + H_2 products reside 50.9 kcal mol^{-1} lower in energy than the initial reactants. Finally, a third, 1,2-H shift in **ma-s5** gives the HCCHCHCCH intermediate **ma-s6** over a barrier of 64.4 kcal mol^{-1}.

The HCCHCHCCH intermediate, 76.3 kcal mol^{-1} below $C_2(^1\Sigma_g^+)$ + CH_3CCH, can split the H atom from C_2 leading to the HCCCHCCH product. As in the case of intermediate **ma-s4**, the endothermicity of the H elimination from **ma-s6** is relatively low, 30.6 kcal mol^{-1}, and the reaction exhibits an exit barrier of 3.9 kcal mol^{-1}. The 2,3-H shift in **ma-s6** occurs via a barrier of 13.5 kcal mol^{-1} and leads to the much more stable C_5H_4 intermediate **ma-s7**, C_{2v}-symmetric $HCCCH_2CCH$, which resides 127.8 kcal mol^{-1} below the reactants. **ma-s7** can fragment by the H loss from C_3 to produce HCCCHCCH without an exit barrier or by H_2 elimination from the same carbon atom to form the bent C_{2v}-symmetric HCCCCCH isomer of C_5H_2 over a barrier of 91.1 kcal mol^{-1}.

In addition to H migrations, C_5H_4 intermediates can rearrange through ring-opening/closure processes (Figure 5b). For instance, **ma-s4** can easily undergo ring closure to **ma-s8** with the barrier and exothermicity of 2.0 and 28.9 kcal mol^{-1}, respectively. A ring closure of structure **ma-s5** leading to intermediate **ma-s9** is less favorable and goes over a barrier of 64.4 kcal mol^{-1}. On the other hand, **ma-s6** is only metastable with respect to the ring closure rearrangement as the barrier separating it from intermediate **ma-s10** is as low as 0.2 kcal mol^{-1}. **ma-s10** can isomerize to a slightly more stable structure by a hydrogen shift between two ring carbons, but the barrier is high, 88.0 kcal mol^{-1}. A similar H shift in **ma-s9** leads to a metastable cyclic intermediate **ma-s11** over a barrier of 58.6 kcal mol^{-1}. Then, **ma-s11** readily ring-opens going over an only 0.1 kcal mol^{-1} barrier and forming a linear cumulenic $H_2CCCCCH_2$ intermediate **ma-s12**. Finally, the cyclic intermediate **ma-s8** can also open its ring and form a branched intermediate **ma-s13**. This process is accompanied by the H shift over the ring C-C bond being cleaved and the formation of a terminal CH_3 group. The **ma-s8** $\rightarrow$ **ma-s13** isomerization is 28.1 kcal mol^{-1} endothermic and exhibits a barrier of 38.6 kcal mol^{-1}.

Now we consider various dissociation pathways of intermediates **ma-s8** - **ma-s13**. **ma-s8** eliminates H_2 from the CH_2 group to form the most stable C_5H_2 isomer ethynylcyclopropenylidene, HC_2-cyc-C_3H. The relative energy of the ethynylcyclopropenylidene + H_2 products is –65.6 kcal mol^{-1} with respect to the initial reactants and the barrier for the dissociation of **ma-s8** is 84.2 kcal mol^{-1}. **ma-s13** can also decompose to the same C_5H_2 isomer by losing H_2 from the CH_3 group overcoming a barrier of 64.2 kcal mol^{-1}. The H_2 elimination process in this case is accompanied by closure of a three-member carbon ring. Structure **ma-s9** can split H_2 from the terminal CH_2 group producing another cyclic C_5H_2 isomer, C_2=cyc-C_3H_2, overcoming a 83.7 kcal mol^{-1} barrier. C_2=cyc-C_3H_2 is 18.9 kcal mol^{-1} less stable than ethynylcyclopropenylidene and

the C_2=cyc-C_3H_2 + H_2 products reside 46.7 kcal mol^{-1} below $C_2(^1\Sigma_g^+)$ + CH_3CCH. The $H_2CCCCCH_2$ intermediate **ma-s12** can either lose a hydrogen atom to form $H_2CCCCCH$ without an exit barrier and with an energy loss of 84.0 kcal mol^{-1} or eliminate H_2 from one of its CH_2 groups giving the H_2CCCCC structure. In the latter case, the reaction proceeds via a barrier of 91.5 kcal mol^{-1} with endothermicity of 77.9 kcal mol^{-1}; the overall $C_2(^1\Sigma_g^+)$ + $CH_3CCH \rightarrow H_2CCCCC + H_2$ reaction is 52.1 kcal mol^{-1} exothermic. No first-order saddle point was found for 1,5-H_2 elimination from two different CH_2 groups in **ma-s12** to produce $HCCCCCH + H_2$; this reaction pathway is clearly unfavorable.

Several dissociation channels leading to the formation of two heavy fragments are also possible but are not favorable thermodynamically. The methyldiacetylene structure **ma-s3** can decompose to CH_3 + linear C_4H ($^2\Sigma^+$) by the cleavage of the terminal H_3C-C single bond. The strength of this bond is calculated to be 132.8 kcal mol^{-1} and the $CH_3 + C_4H$ products are 4.8 kcal mol^{-1} exothermic relative to the initial reactants. A rupture of the C-C single bond in **ma-s4** gives the C_2H_3 + l-C_3H products lying 4.2 kcal mol^{-1} above $C_2(^1\Sigma_g^+)$ + CH_3CCH. The C_3H_3 (propargyl radical) + C_2H (ethynyl radical) products, which lie 18.4 kcal mol^{-1} lower in energy than the reactants, can be formed by the single C-C bond cleavages either in $H_2CCCHCCH$ **ma-s5** or $HCCCH_2CCH$ **ma-s7**. All the fragmentation processes mentioned above take place without exit barriers. Another isomer of C_3H_3, H_3CCC, can be, in principle, produced by the cleavage of the central C-C single bond in methyldiacetylene. However, the H_3CCC structure is known to be ~40 kcal mol^{-1} less stable than the propargyl radical [61] so that the $H_3CCC + C_2H$ product are expected to be about 22 kcal mol^{-1} endothermic. One can see that the single C-C bonds in the C_5H_4 isomers are significantly stronger than most of the C-H bonds and the dissociation processes involving the C-C bond ruptures would not be competitive with H and H_2 eliminations. The reaction pathway leading to the $C_4(^1\Sigma_g^+)$ + CH_4 products starts from the initial three-member ring intermediate **ma-s1**, which undergoes a hydrogen shift between two ring carbons. After the shift depicting a high barrier of 53.1 kcal mol^{-1}, another three-member cyclic local minimum **ma-s15** is produced. **ma-s15** is metastable and can ring-open to the chain intermediate **ma-s16**, $CH_3C(H)CCC$ overcoming a barrier of only 1.5 kcal mol^{-1}. The $CH_3C(H)CCC$ structure is a precursor for CH_4 elimination, which takes place without an exit barrier. The calculated endothermicity of the $C_4(^1\Sigma_g^+)$ + CH_4 products relative to the initial reactants is 2.8 kcal mol^{-1}. The $^1\Sigma_g^+$ state of C_4 is an excited electronic state; the ground $^3\Sigma_g^-$ states lies 10.7 kcal mol^{-1} lower in energy making the $C_4(^3\Sigma_g^-)$ + CH_4 product channel 7.9 kcal mol^{-1} exothermic. However, this channel is spin-forbidden and has to occur via intersystem crossing and therefore is neglected here. The CH_4 loss is not the

only channel for rearrangement or dissociation of $CH_3C(H)CCC$. It can also lose molecular hydrogen to produce $H_2CCCCC + H_2$, but the barrier for the 1,2-H_2 elimination is high and the corresponding transition state lies 8.1 kcal mol^{-1} higher in energy than the $C_2(^1\Sigma_g^+)$ + CH_3CCH reactants. Most likely **ma-s16** would isomerize to the methyldiacetylene structure by the 1,4-H shift overcoming a much lower barrier of 50.7 kcal mol^{-1}.

Only one heavy-fragment decomposition channel might be competitive. It leads to the closed-shell c-C_3H_2 (cyclopropenylidene) + C_2H_2 (acetylene) products, 65.6 kcal mol^{-1} exothermic with respect to $C_2(^1\Sigma_g^+)$ + CH_3CCH, and involves cyclic intermediates **ma-s9** and **ma-s10**. A 1,2-H shift from the terminal CH_2 group in **ma-s9** occurs with a barrier of 69.8 kcal mol^{-1} and leads to another three-member ring intermediate **ma-s14**. It can be also produced from intermediate **ma-s10** by 1,2-H migration from the ring carbon to the neighboring C of the external CCH group. In this case, the barrier with respect to **ma-s10** is 75.6 kcal mol^{-1}. Finally, **ma-s14** dissociates to c-C_3H_2 + C_2H_2 by cleaving the exocyclic C=C double bond and overcoming a barrier of 17.5 kcal mol^{-1}. Interestingly, together with ethynylcyclopropenylidene + H_2, cyclopropenylidene + acetylene are the most exothermic products of the $C_2(^1\Sigma_g^+)$ + CH_3CCH reaction.

In summary, the energized C_5H_4 isomers formed in the reaction of singlet dicarbon with methylacetylene can decompose by H atom eliminations giving the $H_2CCCCCH$ and $HCCCHCCH$ isomers of the C_5H_3 radical, normally, without exit barriers and with overall reaction exothermicity of about 46 kcal mol^{-1}. Second, H_2 eliminations from the C_5H_4 intermediates can lead to a variety of C_5H_2 isomers, including ethynylcyclopropenylidene HC_2-cyc-C_3H, bent $HCCCCCH$, $HCCCHCC$, H_2CCCCC, and C_2=cyc-C_3H_2, for which the reaction exothermicity varies from 65.6 to 46.7 kcal mol^{-1}. Although the H_2 loss channels are more exothermic than H eliminations, all of them take place via exit barriers. The relative energies of transition state corresponding to these barriers are in the range of 20-40 kcal mol^{-1} below the $C_2(^1\Sigma_g^+)$ + CH_3CCH reactants, i.e., they lie higher in energy than the C_5H_3 + H products. Cyclopropenylidene + acetylene are the only highly exothermic heavy-fragment products (-65.6 kcal mol^{-1}) but the transition states corresponding to the highest barriers on the pathways leading to c-C_3H_2 + C_2H_2 lie only 36-37 kcal mol^{-1} lower in energy than the reactants.

5.2. Product branching ratios of the $C_2(^1\Sigma_g^+)$ + $CH_3CCH(^1A_1)$ reaction

In order to quantify branching ratios of various possible C_5H_3 + H, C_5H_2 + H_2, and other products, we carried out microcanonical RRKM calculations of energy-dependent rate constants for individual reaction steps and solved

kinetic equations [59]. In the overall kinetic scheme, we included into our consideration all reaction channels, i.e., H and H_2 eliminations as well as various heavy-fragment formation channels, and assumed that the reaction starts from the energized (chemically-activated) intermediates **ma-s1** and **ma-s2**. The internal energy available to these intermediates equals to the energy of chemical activation, i.e., the well depth at these local minima with respect to the C_2 ($^1\Sigma_g^+$) + CH_3CCH reactants plus collision energy, E_{col}, assuming that the dominant fraction of the latter is converted to the vibrational energy of the intermediates and only a small fraction goes to their rotational excitation. Rate constants were calculated for different collision energies from 0 to 12 kcal mol^{-1}. Since both intermediates **ma-s1** and **ma-s2** can be formed directly from the reactants without a barrier, in the calculations of product branching ratios we considered different relative initial concentrations of **ma-s1** and **ma-s2**, from 100/0 to 0/100. However, the resulting branching ratios appeared to be insensitive to this parameter; both intermediates nearly exclusively isomerize to **ma-s3** because the rate constants for the **ma-s1** $\rightarrow$ **ma-s15** reaction are about four orders of magnitude lower than those for **ma-s1** $\rightarrow$ **ma-s2** and **ma-s2** $\rightarrow$ **ma-s3**, and so the pathway via **ma-s15** cannot compete.

The calculated product branching ratios for E_{col} = 0-12 kcal mol^{-1} are shown in Table 2.

One can see that the dominant reaction products are C_5H_3 radicals + H; the branching ratios of the $H_2CCCCCH$ and HCCCHCCH isomers vary in the ranges of 64-66% and 34-30%, respectively. Most of the $H_2CCCCCH$ radicals, about 72% of their total amount, are produced by H elimination directly from

Table 2. Branching ratios (%) of various products of the $C_2(X^1\Sigma_g^+)$ + $CH_3CCH(X^1A_1)$ reaction.

Products	Collision energy, kJ/mol (kcal mol^{-1})					
	0 (0)	10 (2.39)	20 (4.78)	30 (7.17)	40 (9.56)	50 (11.95)
$H_2CCCCCH$ + H	64.1	64.6	65.0	65.4	65.9	66.2
HCCCHCCH + H	33.8	33.0	32.2	31.4	30.5	29.7
$HCCCCCH$ + H_2	1.2	1.4	1.6	1.9	2.1	2.4
$HCCCHCC$ + H_2	0.6	0.6	0.7	0.7	0.7	0.8
C_2=cyc-C_3H_2 + H_2	4.5×10^{-4}	6.3×10^{-4}	8.7×10^{-4}	0.0	0.0	0.0
HC_2-cyc-C_3H + H_2	0.0	0.0	0.0	0.0	0.0	0.0
H_2CCCCC + H_2	0.0	0.0	0.0	0.0	0.0	0.0
C_3H_3 + C_2H	0.2	0.3	0.4	0.6	0.7	0.9
c-C_3H_2 + C_2H_2	0.0	0.0	0.0	0.1	0.1	0.1
CH_3 + C_4H	1.7×10^{-4}	3×10^{-4}	5.2×10^{-4}	8.3×10^{-4}	0.0	0.0
C_2H_3 + C_3H	0	0.0	0.0	0.0	0.0	0.0
C_4 + CH_4	0	0.0	0.0	0.0	0.0	0.0

methyldiacetylene **ma-s3** and the rest are formed from **ma-s4** and **ma-s5**, about 10% and 18%, respectively. The HCCCHCCH radicals mostly result from the H loss from **ma-s5** (71.7%) and to a less extent from dissociation of **ma-s6** (10.6%) and **ma-s7** (17.7%). The higher yield of the $H_2CCCCCH$ isomer as compared to HCCCHCCH cannot be attributed to the small energetic preference (only 0.3 kcal mol^{-1}) of the former. Actually, the rate constants for the formation of HCCCHCCH from **ma-s5** are slightly higher than for the formation of $H_2CCCCCH$ from the same precursor. The major reason for the higher branching ratio of $H_2CCCCCH$ is that intermediate **ma-s5** yields both $H_2CCCCCH$ and HCCCHCCH, while **ma-s3** yields solely the former, all three dissociation steps having roughly equal rates.

Minor reaction products include HCCCCCH + H_2 (up to 2.4% at the highest collision energy), HCCCHCC + H_2 (up to 0.8%) and, among the heavy-fragment products, C_3H_3 + C_2H (up to 0.9%) and c-C_3H_2 + C_2H_2 (up to 0.1%). However, it would be difficult to detect small amounts of these products experimentally.

5.3. $C_2(^3\Pi_u)$ + $CH_3CCH(^1A_1)$: Triplet potential energy surface and product yields

The calculated potential energy diagram for the $C_2(^3\Pi_u)$ + $CH_3CCH(^1A_1)$ reaction is illustrated in Figure 6. Similar to the reaction of triplet dicarbon with acetylene, the addition of C_2 can occur either to the acetylenic C≡C bond to produce a three-member ring structure or to the individual carbon atoms involved in this bond to form *cis* or *trans* carbon chain adducts. In the case of methylacetylene, two acetylenic C atoms are not equivalent, and so five different addition complexes are possible. Here, we consider only the C_2 addition to the carbon linked to an H atom but not to the methyl group because the reaction pathways are similar in both cases, but slightly more favorable for the C_2 to CH addition rather than for the C_2 to C-CH_3 addition. The addition of dicrabon to the acetylenic bond gives a cyclic intermediate **ma-t1** of C_s symmetry and that to the CH carbon produces $H_3CCC(H)CC$ structures in *trans* (**ma-t2**) and *cis* (**ma-t3**) conformations. All three processes exhibit no entrance barrier and are calculated to be 40.7, 44.3, and 46.2 kcal mol^{-1} exothermic. The three initial intermediates can isomerize to each other by in-plane scrambling of the CH_3 group from *cis* **ma-t3** to *trans* **ma-t2** over a barrier of 7.6 kcal mol^{-1} and by ring closure in **ma-t2** leading to the three-member ring structure **ma-t1** with a barrier of 16.3 kcal mol^{-1}. H elimination from **ma-t2** is unfavorable because it leads to the H_3CCCCC C_5H_3 isomer overcoming a barrier of 40.7 kcal mol^{-1}. H_3CCCCC resides ~36 kcal mol^{-1} higher in energy than the most stable C_5H_3 structures and the overall exothermicity of the H_3CCCCC + H products in the $C_2(^3\Pi_u)$ + $CH_3CCH(^1A_1)$

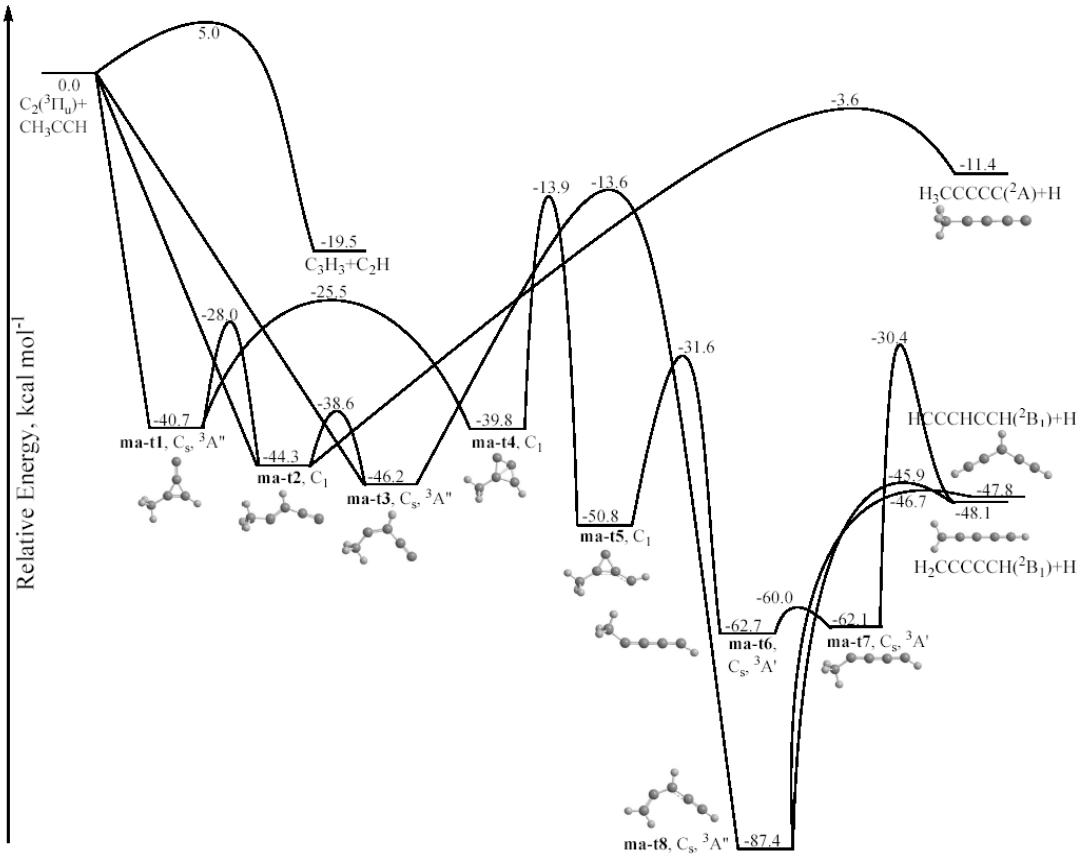

Figure 6. Potential energy diagram of the $C_2(^3\Pi_u)$ + $CH_3CCH(^1A_1)$ reaction.

reaction is only 11.4 kcal mol^{-1}, whereas the exit transition state is located 3.6 kcal mol^{-1} below the reactants.

The three-member ring intermediate **ma-t1** can rearrange to the bicyclic structure **ma-t4** by a second ring closure with a barrier of 15.2 kcal mol^{-1}. Next, **ma-t4** which lies 39.8 kcal mol^{-1} below the reactants can undergo ring opening with a cleavage of the (CH_3)C-CH bond giving another three-member cyclic isomer **ma-t5**, 50.8 kcal mol^{-1} lower in energy than $C_2(^3\Pi_u)$ + $CH_3CCH(^1A_1)$. The barrier for the **ma-t4** → **ma-t5** rearrangement is relatively high, 25.9 kcal mol^{-1}, and the corresponding transition state resides only 13.9 kcal mol^{-1} lower than the reactants. **ma-t5** is a triplet analog of cyclopropenylidene, with two H atoms substituted by CH_3 and CH groups. Opening of the last remaining ring in **ma-t5** leads to the chain isomer $H_3CCCCCH$ in *trans* conformation **ma-t6**, 62.7 kcal mol^{-1} below the reactants, over a barrier of 19.2 kcal mol^{-1}. *Trans-cis* isomerization in $H_3CCCCCH$ leads from **ma-t6** to **ma-t7** with a low barrier of 2.7 kcal mol^{-1}; **ma-t7** is nearly isoergic with **ma-t6**. Finally, *cis* $H_3CCCCCH$ **ma-t7** can eliminate a hydrogen atom from the methyl group giving an i-C_5H_3 radical $H_2CCCCCH$. Our

calculations gave a significant barrier for the H loss from **ma-t7**, 31.7 kcal mol^{-1}. Since the i-C_5H_3 + H products reside 48.1 kcal mol^{-1} below the initial reactants, the reverse barrier for the H addition to the CH_2 group of $H_2CCCCCH$ on the triplet surface is rather high, 17.7 kcal mol^{-1}. Although the $C_2(^3\Pi_u) + CH_3CCH(^1A_1) \rightarrow$ (**ma-t1** ⇆ **ma-t2** ⇆ **ma-t3**) → **ma-t4** → **ma-t5** → **ma-t6** → **ma-t7** → $H_2CCCCCH$ + H reaction mechanism have some similar features with the reaction of triplet dicarbon with acetylene producing C_4H + H, such as analogous entrance channels and isomerization of the initial cyclic adduct to the chain $H_3CCCCCH$ (HCCCCH) structures by ring closure/opening processes through a bicyclic intermediate, there are many differences between the two reactions. First, H loss from the initial chain adducts is clearly unfavorable because a highly excited H_3CCCCC isomer would be formed in this case. Second, H loss occurs specifically from the methyl group because C-H bonds in CH_3 are much weaker than the acetylenic C-H bond. This behavior is reflected in significantly higher exothermicity of the $C_2(^3\Pi_u) + CH_3CCH(^1A_1) \rightarrow H_2CCCCCH$ + H reaction, 48.1 kcal mol^{-1}, as compared to only 10.0 kcal mol^{-1} for $C_2(^3\Pi_u) + C_2H_2 \rightarrow C_4H$ + H. Meanwhile, the unfavorable $C_2(^3\Pi_u) + CH_3CCH(^1A_1) \rightarrow H_3CCCCC$ + H reaction channel exhibits a similar exothermicity (11.4 kcal mol^{-1}) to that of $C_2(^3\Pi_u) + C_2H_2 \rightarrow C_4H$ + H.

Another reaction channel has no analogs in the reaction of triplet dicarbon with acetylene. It starts from **ma-t3** and proceeds by 1,5-H migration from the methyl group to the terminal carbon atom over a barrier of 32.6 kcal mol^{-1}. This leads to a very stable chain isomer $H_2CCC(H)CCH$ **ma-t8**, residing 87.4 kcal mol^{-1} below the initial reactants and about 25 kcal mol^{-1} lower in energy than the $H_3CCCCCH$ structures **ma-t6** and **ma-t7**. Two different H eliminations are feasible from **ma-t8**: the loss from the CH_2 group leads to n-C_5H_3 [HCCC(H)CCH] + H with a barrier 40.7 kcal mol^{-1}, whereas the H loss of the central hydrogen gives i-C_5H_3 + H with a similar barrier of 41.5 kcal mol^{-1}. In this case, the reverse barriers for H addition to the C_5H_3 isomers are low, only 1.1 and 2.2 kcal mol^{-1}. It is important to elucidate whether the reaction preferably proceeds via **ma-t4** – **ma-t7** or **ma-t3** and **ma-t8**, because this would have important consequences for the reaction dynamics and the product yield. If the decomposing complex is **ma-t7**, the dominating reaction product should be i-C_5H_3 and the high exit barrier should be reflected in translational energy distribution of the products. Otherwise, the decomposing **ma-t8** complex would lead to comparable yields of i- and n-C_5H_3 isomer over rather low exit barriers. Since under single collision conditions of crossed molecular beam experiments all intermediates maintain the energy of chemical activation (plus collision energy), the critical transition transition states for the $C_2(^3\Pi_u) + CH_3CCH(^1A_1) \rightarrow$ (**ma-t1** ⇆ **ma-t2** ⇆ **ma-t3**) → **ma-t4** → **ma-t5** →

ma-t6 → **ma-t7** → $H_2CCCCCH$ + H and $C_2(^3\Pi_u)$ + $CH_3CCH(^1A_1)$ → (**ma-t1** ⇆ **ma-t2** ⇆ **ma-t3**) → **ma-t8** → $H_2CCCCCH$ + H / HCCC(H)CCH + H mechanisms are those which have highest relative energies with respect to the initial reactants. These rate determining transition states are TSs for **ma-t4** → **ma-t5** (-13.9 kcal mol^{-1}) and **ma-t3** → **ma-t8** (-13.6 kcal mol^{-1}), respectively, which lie much higher in energy than all other transition states, including those for the H losses. In order to evaluate relative importance of the two reaction channels, we calculated RRKM rate constants for the processes starting from the common intermediate **ma-t3** and passing through the critical transition states. The results show that the reaction leading to i-C_5H_3 + H via the **ma-t4** → **ma-t5** TS is 6.2 times faster than that leading to i-C_5H_3/n-C_5H_3 + H via TS **ma-t3** → **ma-t8** at collision energies of 0-12 kcal mol^{-1}. Although the two critical transition states have similar energies, the **ma-t4** → **ma-t5** TS involving a ring opening process is much looser than the **ma-t3** → **ma-t8** TS for H migration. Indeed, the four lowest calculated real vibrational frequencies for the former are 152, 228, 264, and 356 cm^{-1} as compared to 316, 388, 408, and 483 cm^{-1} for the latter. This makes the number of vibrational states for the **ma-t4** → **ma-t5** TS significantly higher than that for the **ma-t3** → **ma-t8** TS and thus leads to higher rate constants for the former process. As a result, the pathway via **ma-t4** → **ma-t5** to **ma-t7** is significantly more favorable than that via **ma-t3** → **ma-t8**, 86% vs. 14%, and we expect that i-C_5H_3 formed by H elimination from **ma-t7** should be the dominant reaction product.

No pathways leading to C_5H_2 triplet isomers by H_2 elimination have been found. Also, most of the reaction channels leading to spin-allowed heavy fragments (radical + radical) are energetically unfavorable (see Section 5.1), except for the propargyl, $C_3H_3(^2B_1)$, plus ethynyl, $C_2H(^2\Sigma^+)$, pair exothermic by 19.5 kcal mol^{-1}. In the region of triplet C_5H_4 PES probed by the $C_2(^3\Pi_u)$ + CH_3CCH reaction, no precursor exists which can directly dissociate to C_3H_3 + C_2H. However, these products can be formed by the direct H abstraction by triplet C_2 from the CH_3 group of methylacetylene. The H abstraction barrier is calculated to be 5.0 kcal mol^{-1}, and, although this process is clearly less favorable than the barrierless C_2 addition to the acetylenic bond, it might contribute at higher collision energies.

5.4. Comparison with experimental results

Experimentally, the reaction dynamics of C_2 in the $^1\Sigma_g^+$ and $^3\Pi_u$ first electronic states with methylacetylene were investigated under single collision conditions utilizing the crossed molecular beam approach at four collision energies between 3.3 and 12.0 kcal mol^{-1} [25,62]. The results suggested that the reactions proceed via indirect scattering dynamics and involve two channels on the singlet and one channel on the triplet potential energy surface.

In the singlet state, the initial collision complexes isomerize forming eventually a methyldiacetylene intermediate, which either decomposes to the 2,4-pentadiynyl-1 radical [i-C_5H_3(X^2B_1), $HCCCCCH_2$] or rearranges to ethynyl allene ($H_2CCCHCCH$) through two successive hydrogen shifts. This structure fragments then to i-C_5H_3 or 1,4-pentadiynyl-3 radical [n-C_5H_3 (X^2B_1) HCCCHCCH]. These conclusions are in line with the results of our calculations of the product branching ratios, which gave i-C_5H_3 and n-C_5H_3 as the dominant reaction products with the ratio of 2:1, where the former is mostly formed from methyldiacetylene **ma-s3** (72%), and ~72% of the latter are produced from ethynyl allene **ma-s5**. On the triplet surface, the initial collision complexes isomerize yielding ultimately cis-methyldiacetylene; this isomer fragmented via a tight exit transition state to the 2,4-pentadiynyl-1 radical, i-C_5H_3. The assessment of the center-of-mass translational energy distributions implied that the formation of the C_5H_3 radical(s) and atomic hydrogen is exoergic by 43.3±2.9 kcal mol^{-1}, which agrees fairly well with the calculated exothermicities of ~46 and ~48 kcal mol^{-1} for the singlet and triplet reactions, respectively. No products other than C_5H_3 + H were detected experimentally; again, this in agreement with the theoretical results that at most 2-3% of C_5H_2 + H_2 can be formed in the singlet reaction, that no H_2 elimination pathway was identified in the triplet state, and that fragmentation of singlet or triplet C_5H_4 to two heavy fragments is clearly unfavorable.

The conclusions above were also supported by an experiment utilizing partially deuterated methylacetylene, CD_3CCH [25,62]. Here, the decomposition of a CD_3C_4H intermediate (m/z = 67) could form CD_2C_4H (D atom loss; m/z = 65) or C_5D_3 (m/z = 66; H atom loss). Experimentally, only signal at m/z = 65 was observed, but not at m/z = 66. This verified explicitly that the released atom is a deuterium atom. On the singlet surface, i-C_5H_3 can be formed from **ma-s3**, **ma-s4**, and **ma-s5** and in all three cases elimination of a D atom initially from the CD_3 group is involved. On the other hand, the branching ratio calculations showed that n-C_5H_3 is produced from **ma-s5**, **ma-s6**, and **ma-s7** and again these processes can occur only by D elimination, if CD_3CCH is the initial reactant. The CD_3-C≡C-C≡C-H structure could also be a precursor of $D_3CCCCC(X^2A)$, however, this C_5H_3 isomer resides 36.6 kcal mol^{-1} above D_2CCCCH and its formation is clearly unfavorable. On the triplet surface, H elimination could be observed only if **ma-t8** would be the decomposing complex; **ma-t7** can dissociate by D elimination because the CD_3 group remains intact along this pathway. The non-observation of the H loss confirms the results of RKKM calculations that the reaction mechanism via **ma-t7** is ~6 times faster than via **ma-t8**. Although a minor amount (~14%) of C_5H_3 products could be formed from **ma-t8**, they were not detected in experiment.

The identification of two resonance-stabilized free C_5H_3 radicals, i.e. 2,4-pentadiynyl-1 (singlet and triplet surface) and 1,4-pentadiynyl-3 (singlet surface), in the reaction of dicarbon with methylacetylene suggests that both molecules can be important transient species in the chemical evolution of the interstellar medium and in combustion flames; here, a reaction with the methyl radical (CH_3) could access the important C_6H_6 potential energy surface [60].

6. Reactions of C_2 with allene

6.1. $C_2(^1\Sigma_g^+)$ + $CH_2CCH_2(^1A_1)$: Singlet potential energy surface and product yields

The reaction of singlet dicarbon with allene involves the same C_5H_4 potential energy surface as the reaction with methylacetylene, however, accesses a rather different area on this surface (Figure 7). Similar to the reaction of singlet C_2 with ethylene, the dicarbon molecule adds to the double bond of allene without a barrier to produce a C_s-symmetric three-member ring intermediate **al-s1** residing 83.4 kcal mol^{-1} below the initial reactants (compare with **et-s1** lying 85.5 kcal mol^{-1} lower in energy than $C_2(^1\Sigma_g^+)$ + C_2H_4). The initial complex transforms into the linear singlet pentatetraene isomer **al-s2** after overcoming a barrier of 13.4 kcal mol^{-1}, which is very similar to the barrier for the analogous **et-s1** → **et-s2** (butatriene) isomerization on the C_4H_4 PES, 14.2 kcal mol^{-1}. Pentatetraene **al-s2** residing 130.6 kcal mol^{-1} lower in energy than $C_2(^1\Sigma_g^+)$ + CH_2CCH_2 has been already identified earlier in Section 5.1 and was denoted as **ma-s12**. Pentatetraene can decompose through two different channels, H elimination without an exit barrier producing i-C_5H_3 lying 46.6 kcal mol^{-1} lower in energy than the reactants and 1,1-H_2 loss giving H_2CCCCC, 52.7 kcal mol^{-1} below $C_2(^1\Sigma_g^+)$ + C_2H_4. The barrier for the H_2 elimination is 91.5 kcal mol^{-1}. An alternative for the decomposition of **al-s2** is its isomerization to **al-s5** (**ma-s5**) by a three-member ring closure to **al-s3** (**ma-s11**), 1,2-H migration to **al-s4** (**ma-s9**) completed by the ring opening. The highest barrier on the **al-s2** → **al-s5** pathway is 81.8 kcal mol^{-1} relative to pentatetraene (between **al-s3** and **al-s4**), however, the corresponding TS involves H migration and is tight. From **al-s5** (**ma-s5**) the system accesses the regions of the C_5H_4 singlet PES described in Section 5.1 for the singlet C_2 + methylacetylene reaction. However, according to our RRKM calculations of reaction rate constants, the probability of this to happen is very low. In particular, the computed rate for isomerization of pentatetraene **al-s2** to ethynyl allene **ma-s5** is 60-63 times lower than the overall rate constant for its dissociation through the H and H_2 loss channels at collision energies of 0-12 kcal mol^{-1}, so that less than 1-2% of reaction products can be formed via the pathway involving **ma-s5**.

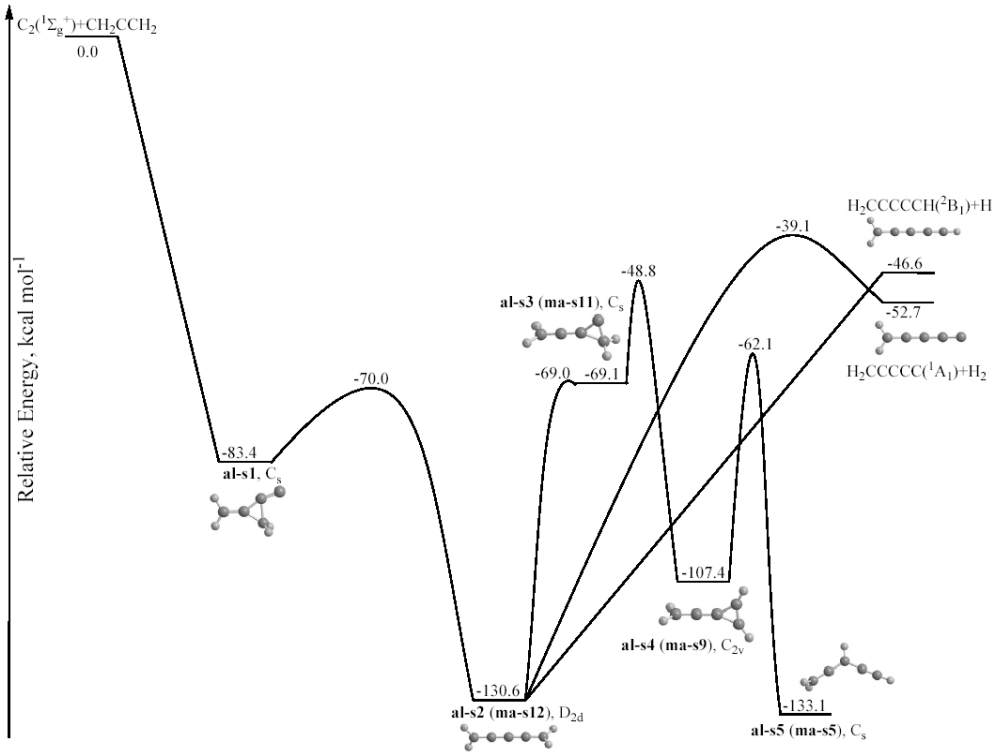

Figure 7. Potential energy diagram of the $C_2(^1\Sigma_g^+) + CH_2CCH_2(^1A_1)$ reaction.

We can conclude that pentatetraene **al-s2** is the main decomposing complex in the $C_2(^1\Sigma_g^+) + CH_2CCH_2$ reaction. A comparison of the H and H_2 elimination rate constants from **al-s2** gives the i-C_5H_3 + H and H_2CCCCC + H_2 branching ratios as 98% and 2%, respectively. Thus, the calculations predict i-C_5H_3 to be the dominant reaction product, whereas small amounts of H_2CCCCC may also be formed.

6.2. $C_2(^3\Pi_u)$ + $CH_2CCH_2(^1A_1)$: Triplet potential energy surface and product yields

The reaction scenario in triplet state (Figure 8) appears to be more complicated. Initial addition of $C_2(^3\Pi_u)$ can occur not only to a terminal carbon of allene involved in a CH_2 group but also to the central carbon atom. When dicarbon adds to a CH_2 carbon, first steps of the reaction mechanism are similar to those of the $C_2(^3\Pi_u)$ + C_2H_4 reaction (Section 4.3). Initially, the reactants recombine without a barrier producing a H_2CCCH_2CC intermediate **al-t1** residing 36.4 kcal mol^{-1} below the reactants – compare with 30.2 kcal mol^{-1} for **et-t1** in the ethylene reaction. **al-t1** rearranges to a three-member ring intermediate **al-t2** (29.3 kcal mol^{-1} lower in energy than $C_2(^3\Pi_u)$ + CH_2CCH_2) by ring closure over a relatively low barrier of 12.8 kcal mol^{-1}, which is slightly higher than the barrier for the analogous **et-t1** → **et-t2** isomerization

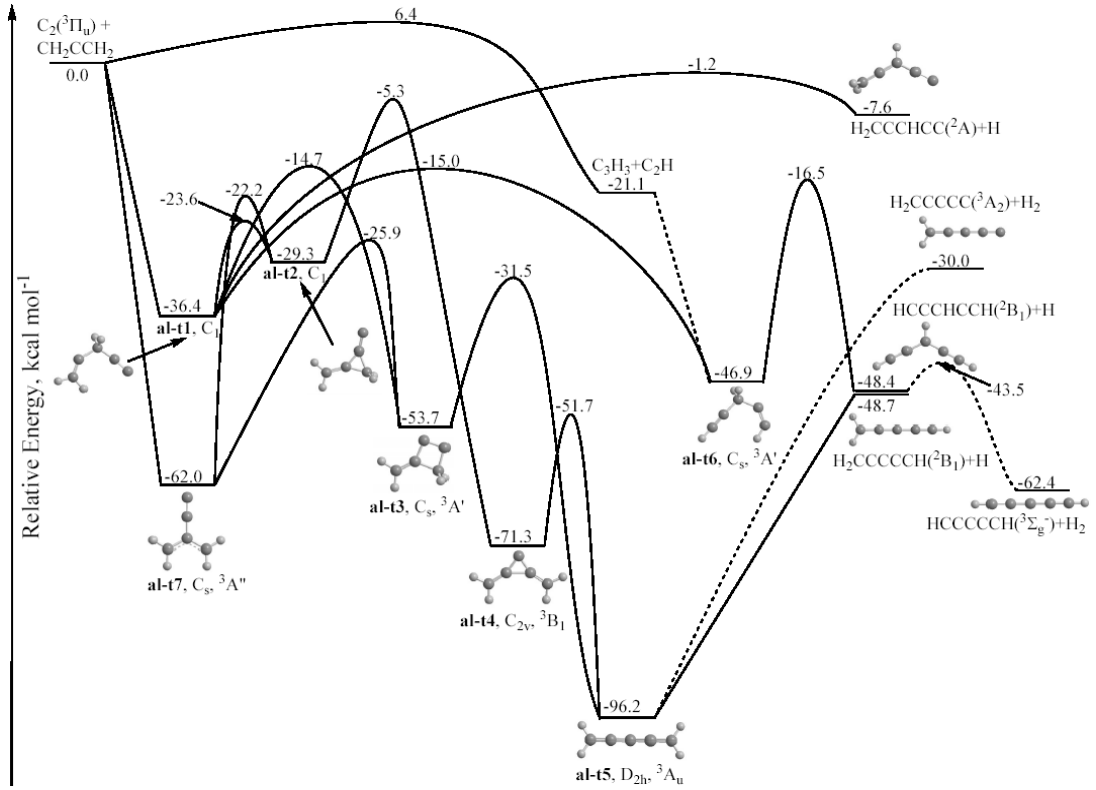

Figure 8. Potential energy diagram of the $C_2(^3\Pi_u)$ + $CH_2CCH_2(^1A_1)$ reaction.

on the triplet C_4H_4 surface, 9.4 kcal mol^{-1}. Four-member ring closure in **al-t1** can lead to another, more stable cyclic intermediate **al-t3** (-53.7 kcal mol^{-1} relative to the reactants) via a higher barrier of 21.7 kcal mol^{-1}. In the ethylene system, the four-member ring closure from **et-t1** to **et-t3** exhibits a lower barrier of 15.0 kcal mol^{-1}. Opening of the four-member cycle in **al-t3** leads to the triplet pentatetraene isomer **al-t5**, which lies 96.2 kcal mol^{-1} below $C_2(^3\Pi_u)$ + CH_2CCH_2. The **al-t3** $\rightarrow$ **al-t5** ring-opening barrier is calculated to be 22.2 kcal mol^{-1}, close to the barrier for the similar **et-t3** $\rightarrow$ **et-t7** process for triplet C_4H_4. Next, triplet pentatetraene **al-t5** can lose a hydrogen atom to produce i-C_5H_3 with endothermicity of 47.5 kcal mol^{-1}. Although a low exit barrier for the H elimination was found at the B3LYP/6-311G** level, it disappears within the more accurate G2M(MP2) computational approach. Note that on the triplet C_4H_4 PES, the H loss from the butatriene intermediate **et-t7** is endothermic by 53.7 kcal mol^{-1} and exhibits a low exit barrier of 2.2 kcal mol^{-1}.

Here, however, the analogy between the $C_2(^3\Pi_u)$ reactions with ethylene and allene ends, as the presence of an extra carbon atom makes the triplet C_5H_4 PES more complex. For instance, 1,5-H migration in **al-t1** can lead to another chain structure $HCCCH_2CCH$ **al-t6** (46.9 kcal mol^{-1} below the reactants) overcoming a barrier of 21.4 kcal mol^{-1}. **al-t6** can eliminate an H atom from

the central CH_2 group to produce the n-C_5H_3 radical. In this case, the **al-t6** → n-C_5H_3 + H process is 1.5 kcal mol^{-1} exothermic and the barrier for the H loss is high, 30.4 kcal mol^{-1}. Intermediate **al-t2** can rearrange to another three-member ring isomer **al-t4** trough a ring closure/ring opening process with a bicyclic transition state over a barrier of 24.0 kcal mol^{-1}. **al-t4** has a highly symmetric C_{2v} geometry with two CH_2 groups attached to the C_3 ring and resides 71.3 kcal mol^{-1} below $C_2(^3\Pi_u)$ + CH_2CCH_2. Three-member ring opening in **al-t4** produces triplet pentatetraene **al-t5** after overcoming a 19.6 kcal mol^{-1} barrier. Alternatively, **al-t2** can ring open to a branched C_{2v}-symmetric intermediate **al-t7** with a barrier of only 7.1 kcal mol^{-1}. The structure **al-t7** itself can be formed directly from the initial $C_2(^3\Pi_u)$ + CH_2CCH_2 reactants by barrierless addition of the triplet dicarbon molecule to the central C atom of allene. Actually, the C_2 addition to the central carbon is more favorable energetically than the addition to a terminal C atom; **al-t7** lies 62.0 kcal mol^{-1} lower in energy than the reactants and 34.4 kcal mol^{-1} below the other initial adduct **al-t1**. **al-t7** can undergo either a three-member closure to **al-t2** with a barrier of 39.8 kcal mol^{-1} or a four-member ring closure to **al-t3** over a slightly lower barrier of 36.1 kcal mol^{-1}. At these stages, the reaction channels which start from **al-t1** and **al-t7** merge.

It should be noted that the reaction channels connecting the region of the triplet C_5H_4 PES accessed by the $C_2(^3\Pi_u)$ + allene reaction with that probed in the reaction of triplet dicarbon with methyl acetylene (Section 5.3) are not favorable. For instance, intermediate **ma-t3** can be obtained from **al-t1** by two consecutive 1,2-H migrations but the corresponding barriers are high, in the range of 33 kcal mol^{-1}. This is at least ~10 kcal mol^{-1} higher than the barriers for the other rearrangements of **al-t1**, which do not involve hydrogen shifts, making the **al-t1** → **ma-t3** isomerization unlikely. **al-t4** can be transformed to **ma-t5** by H migration from one CH_2 group to another, but again the respective barrier is high, ~72 kcal mol^{-1}, more than 50 kcal mol^{-1} higher than the barrier for the **al-t4** → **al-t5** ring opening step. We can conclude that, because any rearrangement between the allene- and methylacetylene-related regions of the surface will necessarily require H migration processes characterized by high barriers and tight transition states, the two reactions of triplet dicarbon are not likely to pass through a common intermediate.

In summary, three reaction channels should lead to the formation of the i-C_5H_3 + H products, including $C_2(^3\Pi_u)$ + CH_2CCH_2 → **al-t1** → **al-t2** → **al-t7** → **al-t3** → **al-t5** → i-C_5H_3 + H with the rate-determining transition state between **al-t2** and **al-t7** lying 22.2 kcal mol^{-1} below the reactants, **al-t1** → **al-t3** → **al-t5** → i-C_5H_3 + H (the critical TS is between **al-t1** and **al-t3**, 14.7 kcal mol^{-1} lower in energy than $C_2(^3\Pi_u)$ + CH_2CCH_2), and $C_2(^3\Pi_u)$ + CH_2CCH_2 → **al-t7** → **al-t3** → **al-t5** → i-C_5H_3 + H (TS between **al-t7** and **al-t3**, 25.9 kcal

mol^{-1} below the reactants). The other isomer of the C_5H_3 radical, n-C_5H_3, can be formed from the initial adduct **al-t1** by the **al-t1** → **al-t6** → n-C_5H_3 + H mechanism with the rate-controlling TS for the H shift between **al-t1** and **al-t6** lying 15.0 kcal mol^{-1} below $C_2(^3\Pi_u)$ + CH_2CCH_2. If the **al-t7** adduct is produced initially, in order to reach the n-C_5H_3 + H products it will have to first isomerize to **al-t1** via **al-t2**. To compare relative importance of the three channels involving the common intermediate **al-t1**, **al-t1** → **al-t2** → **al-t7** → **al-t3** → **al-t5** → i-C_5H_3 + H, **al-t1** → **al-t3** → **al-t5** → i-C_5H_3 + H, and **al-t1** → **al-t6** → n-C_5H_3 + H, we evaluated their RRKM rate constants assuming that one step in each mechanism, which has highest in energy transition state (**al-t2** → **al-t7**, **al-t1** → **al-t3**, and **al-t1** → **al-t6**, respectively) is rate-determining. The calculations showed that the channel leading to the i-C_5H_3 products via **al-t7** is clearly dominant (97-93% at the collision energies of 0-12 kcal mol^{-1}). The pathway leading to the same products via **al-t3** and **al-t5** bypassing **al-t7** contributes 2-4%, whereas the channel producing n-C_5H_3 via **al-t6** gives only 1-2%, although its role slightly increases with the collision energy. We conclude that, if the reaction to follow a statistical behavior, the dominant products should be i-C_5H_3 + H produced by decomposition of the symmetric triplet pentatetraene intermediate **al-t5**. A minor amount of the n-C_5H_3 + H products may be formed from the low-symmetry **al-t6** precursor.

No reaction products other than C_5H_3 + H are expected to be produced in the $C_2(^3\Pi_u)$ + CH_2CCH_2 reaction in significant amounts. The **al-t5** isomer could, in principle, serve as a precursor for one-center H_2 elimination. However, this process leading to the $H_2CCCCC(^3A_2)$ + H_2 products is computed to be 66.2 kcal mol^{-1} endothermic, i.e., 18.7 kcal mol^{-1} less favorable than the H loss leading to $H_2CCCCCH(^2B_1)$ + H, and therefore is not expected to be competitive. A search of a transition state for 1,1-H_2 elimination from **al-t6** converged instead to a TS for H atom abstraction from the n-C_5H_3 isomer, $HCCCHCCH(^2B_1)$ + H → $HCCCCCH(^3\Sigma_g^-)$ + H_2. Although the $HCCCCCH(^3\Sigma_g^-)$ + H_2 products are found to be exothermic by 62.4 kcal mol^{-1}, i.e., 13.7 kcal mol^{-1} more stable than i-C_5H_3 + H, they can be formed only in secondary reactions of C_5H_3 radicals with H atoms; this cannot happen under single collision conditions. Among spin-allowed heavy fragment products, propargyl radical, $C_3H_3(^2B_1)$, plus ethynyl radical, $C_2H(^2\Sigma^+)$, are the most exothermic, as they lie 21.1 kcal mol^{-1} below the reactants. A C-C bond cleavage in **al-t6** can lead to these products, however, since the reaction channel passing through this intermediate is minor, only small amounts of C_3H_3 + C_2H can be produced by its decomposition. Alternatively, C_3H_3 + C_2H can be formed by the direct H abstraction by triplet dicrabon from allene. The H abstraction barrier is calculated to be 6.4 kcal mol^{-1}, so that this process is not likely to compete with the barrierless and strongly exothermic C_2 additions, at least, at low collision energies.

6.3. Comparison with experimental results

The reactions dynamics of singlet and triplet dicarbon molecules C_2 with allene were investigated experimentally under single collision conditions using the crossed molecular beam approach at four collision energies between 3.3 and 11.8 kcal mol^{-1} [63]. The results showed that the reactions are barrierless and indirect on both the singlet and the triplet surfaces and proceed through bound C_5H_4 intermediates via addition of the dicarbon molecule to the carbon-carbon double bond (singlet surface) and to the terminal as well as central carbon atoms of the allene molecule (triplet surface). The initial collision complexes isomerize to form triplet and singlet pentatetraene intermediates ($H_2CCCCCH_2$) which decompose via atomic hydrogen loss to yield the 2,4-pentadiynyl-1 radical i-C_5H_3, $HCCCCCH_2(X^2B_1)$. These channels result in symmetric center-of-mass angular distributions. The measured translational energy distribution indicated that the formation of the C_5H_3 + H products is exothermic by 45.7±2.6 kcal mol^{-1}, in good agreement with the calculated values of ~47 and ~49 kcal mol^{-1} for the singlet and triplet reactions, respectively. A second product channel had also to be invoked to account for the observed backward-scattered center-of-mass angular distributions at higher collision energies. The only plausible candidate for this channel is decomposition of a non-symmetric reaction intermediate ($HCCCH_2CCH$, **al-t6**), which belongs to the C_s point group and hence holds no C_2 rotational axis, through atomic hydrogen emission to the 1,4-pentadiynyl-3 radical [n-$C_5H_3(X^2B_1)$, HCCCHCCH] on the triplet surface. Although this channel appears to be minor according to our RRKM calculations, it may break the symmetry of the center-of-mass angular distributions at higher collision energies, where its contribution increases to up to 2%. It is also conceivable that some dynamical (non-statistical) effects may enhance the production of the **al-t6** intermediate and consequently of the n-C_5H_3 + H (and possibly, C_3H_3 + C_2H) products.

7. Conclusions and implications

Potential energy surfaces for the reactions of dicarbon molecules in the ground singlet $^1\Sigma_g^+$ and first excited triplet $^3\Pi_u$ electronic states with simplest unsaturated hydrocarbons acetylene, ethylene, methylacetylene, and allene have been studied using high level ab initio G2M(MP2)/B3LYP/6-311G** and CCSD(T)/6-311+G(3df,2p)/B3LYP/6-311G** calculations. The results show that C_2 adds to double and triple bonds of unsaturated hydrocarbons without a barrier yielding initially acyclic (triplet surface) as well as three- and four-membered cyclic adducts (triplet and singlet surfaces) C_4H_2, C_4H_4, and C_5H_4. After the formation of these initial complexes, the reactions proceed by C_2 insertion into the attacked C-C bond followed by isomerizations involving ring

opening/ring closure processes and hydrogen migrations. In particular, the cyclic structures isomerize to form eventually diacetylene (HCCCCH; C_2/C_2H_2), butatriene (H_2CCCCH_2; C_2/C_2H_4), methyldiacetylene (CH_3CCCCH; C_2/CH_3CCH), and pentatetraene ($H_2CCCCCH_2$; C_2/H_2CCCH_2) intermediates on the singlet surface or their counterparts in the triplet state. Under single collision conditions, the C_4H_2, C_4H_4, and C_5H_4 species can dissociate through a loss of a hydrogen atom, H_2 molecule, or decompose to a pair of heavy fragments. According to RRKM calculations of reaction rate constants and product branching ratios, the dominant channels for the most reactions considered here (except $C_2(^1\Sigma_g^+)$ + C_2H_4) are H eliminations producing 1,3-butadiynyl [$C_4H(X^2\Sigma^+)$ HCCCC], 1-butene-3-yne-2-yl [i-$C_4H_3(X^2A'')$ H_2CCCCH], 2,4-pentadiynyl-1 [i-C_5H_3 (X^2B_1) $HCCCCCH_2$], and possibly 1,4-pentadiynyl-3 radical [n-$C_5H_3(X^2B_1)$ HCCCHCCH]. These findings agree with the results of crossed molecular beams experiments on the reactions considered here, which gave only C_4H, C_4H_3, and C_5H_3 products. The calculations and experiments are also in agreement that molecular hydrogen pathways are unimportant and may provide only a minor fraction of the total reaction products. In the reaction of singlet dicrabon with ethylene at low collision energies, the branching ratio of the C_2H_2 + CCH_2 heavy fragment can reach nearly 50% and to be somewhat higher than the branching ratio of i-C_4H_3 + H, however, the latter steadily increases with the collision energy. Although the C_2H_2 + CCH_2 products were not detected in the crossed molecular beams studies, acetylene was found in thermal decomposition of vinylacetylene C_4H_4 [58] occurring in the electronic ground state on the same singlet C_4H_4 PES. In general, the reaction products and their relative yields are summarized by the following equations:

$C_2(^1\Sigma_g^+/^3\Pi_u) + C_2H_2 \rightarrow HCCCC\ (^2\Sigma^+) + H$

$C_2(^1\Sigma_g^+) + C_2H_4 \rightarrow$ i-C_4H_3 + H / C_2H_2 + H_2CC / minor C_4H_2 + H_2

$C_2(^3\Pi_u) + C_2H_4 \rightarrow$ i-C_4H_3 + H / trace n-C_4H_3 + H

$C_2(^1\Sigma_g^+) + H_3CCCH \rightarrow$ i-C_5H_3 ($H_2CCCCCH$) + H / n-C_5H_3 (HCCCHCCH) + H (2:1)

$C_2(^3\Pi_u) + H_3CCCH \rightarrow$ i-C_5H_3 ($H_2CCCCCH$) / minor n-C_5H_3 (HCCCHCCH) + H

$C_2(^1\Sigma_g^+) + H_2CCCH_2 \rightarrow$ i-C_5H_3 ($H_2CCCCCH$) + H / minor C_5H_2 + H_2

$C_2(^3\Pi_u) + H_2CCCH_2 \rightarrow$ i-C_5H_3 ($H_2CCCCCH$) + H / minor n-C_5H_3 (HCCCHCCH) + H

The overall reactions to form the hydrogen-deficient radicals C_4H, C_4H_3, and C_5H_3 were found to be exoergic and the calculated reaction energies agree with the exothermicities deduced from experimental translational energy distributions within the error bars of 1-3 kcal mol^{-1}. The underlying characteristics (indirect scattering dynamics; no entrance barrier; isomerization

barriers below the energy of the separated reactants; exoergic reactions) suggests the enormous potential of the dicarbon plus unsaturated hydrocarbon reaction class to form highly hydrogen-deficient carbonaceous molecules in cold molecular clouds and in circumstellar envelopes of carbon stars. In denser environments such as in comets and related oxygen-poor combustion flames, the identified reaction intermediates can also be stabilized via a third body collision.

All radicals formed in the C_2 reactions described here are expected to play a significant role in formation of aromatic ring(s) in extraterrestrial environments. The 2,4-pentadiynyl-1 radical represents also an important resonance-stabilized free radical [60,64]; compared to the propargyl radical [$HCCCH_2(X^2B_1)$] – thought to be a major growth species to form the very first aromatic ring in oxygen-poor and hydrocarbon rich environments - the 2,4-pentadiynyl-1 radical is expanded by one carbon-carbon triple bond to give rise to a linear heavy carbon atom backbone and its reaction with the methyl radical may efficiently produce benzene or phenyl radical plus atomic hydrogen [65]. Therefore, the inclusion of the reaction products of these neutral-neutral reactions into astrochemical models of carbon rich circumstellar envelopes and molecular clouds will lead to a refined understanding on the formation of polycyclic aromatic hydrocarbons, their hydrogen deficient precursors, and of carbon-rich nanostructures. Our examinations hold also strong ties to combustion processes in oxygen-poor hydrocarbon flames [65]. Astrophysicists and combustion chemists have utilized comparable reaction networks to model the chemistry of interstellar and flame environments; multi-component models of carbon cluster growth and the correlation with PAHs and soot formation are typical cases involving highly reactive carbon chains and hydrogen-deficient hydrocarbon radicals such as 1,3-butadiynyl [$C_4H(X^2\Sigma^+)$ HCCCC] and most important the 1-butene-3-yne-2-yl radical [i-$C_4H_3(X^2A')$ H_2CCCCH] [66-75]. Therefore, our findings can also help to shed light in explaining the formation of these radicals in oxygen-poor combustion flames. In denser environments like combustion processes, the internally excited intermediates of the reactions of dicarbon with the hydrocarbon molecules can be stabilized via a third body reaction. This effectively diverts (a fraction of) the excess energy from the intermediates to the third body thus stabilizing the intermediates involved. Note that these processes are not important in cold molecular clouds and in the outer regions of the circumstellar envelopes where solely bimolecular reactions prevail. Therefore, the chemistry of hydrocarbon flames is clearly more complicated; future chemical models of oxygen-poor combustion flames should therefore also incorporate the reaction intermediates involved in the present studies to yield a complete picture on the formation of hydrogen-poor carbonaceous molecules in these environments.

Acknowledgements

This work was supported by the Chemical Sciences, Geosciences and Biosciences Division, Office of Basic Energy Sciences, Office of Sciences of the U.S. Department of Energy (Grant No. DE-FG02-04ER15570 to FIU and Grant No. DE-FG02-03ER15411 to the University of Hawaii).

References

1. Faraday Discussion 119, Combustion Chemistry: Elementary Reactions to Macroscopic Processes, 2001.
2. R. D. Kern, K. Xie, H. Chen, Combust. Sci. Technol. **85**, 77 (1992).
3. J. H. Kiefer, S. S. Sidhu, R. D. Kern, K. Xie, H. Chen, L. B. Harding, Combust. Sci. Technol. **82**, 101 (1992).
4. C. E. Baukal, *Oxygen-enhanced combustion*, CRS Press, New York, 1998.
5. Y. C. Minh, E. F. Dishoeck, *Astrochemistry – From Molecular Clouds to Planetary Systems*. ASP Publisher, San Francisco, 2000.
6. Faraday Discussion 109, *Chemistry and Physics of Molecules and Grains in Space*, 1998.
7. H. J. Fraser, M. R. S. McCoustra, D. A. Williams, Astron. Geophys. **43**, 10 (2002).
8. R. I. Kaiser, C. Ochsenfeld, D. Stranges, M. Head-Gordon, Y. T. Lee, Faraday Discuss. **109**, 183 (1998).
9. C. C. Chiong, O. Asvany, N. Balucani, Y. T. Lee, R. I. Kaiser, *Nucleation of hydrogen deficient carbon clusters in circumstellar envelopes of carbon stars.* World Scientific Press, Proceedings of the 8th Asia-Pacific Physics Conference, APPC 2000, 2001, 167.
10. R. I. Kaiser, N. Balucani, Int. J. Astrobiol. **1**, 15 (2002).
11. J. Appel, H. Bockhorn, M. Frenklach, Combust. Flame **121**, 122 (2000).
12. A. Kazakov, M. Frenklach, Combust. Flame **114**, 484 (1998).
13. A. Kazakov, M. Frenklach, Combust. Flame **112**, 270 (1998).
14. L. Vereecken, H. F. Bettinger, J. Peeters, Phys. Chem. Chem. Phys. **4**, 2019 (2002).
15. P. Ehrenfreund, S. B. Charnley, Annu. Rev. Astron. Astrophys. **38**, 427 (2000).
16. H. Richter, O. A. Mazyar, R. Sumathi, W. H. Green, J. B. Howard, J. W. Bozzelli, J. Phys. Chem. A **105**, 1561 (2001).
17. W. M. Pitts, L. Pasternack, J. R. McDonald, Chem. Phys. **68**, 417 (1982).
18. L. Pasternack, W. M. Pitts, J. R. McDonald, Chem. Phys. **57**, 19 (1981).
19. V. M. Donnely, L. Pasternack, Chem. Phys. **39**, 427 (1979).
20. L. Pasternack, J. R. McDonald, Chem. Phys. **43**, 173 (1979)
21. H. Reisler, M. Mangir, C. Wittig, J. Chem. Phys. **71**, 2109 (1979).
22. K. H. Becker, B. Donner, H. Geiger, F. Schmidt, P. Wiesen, Z. Phys. Chem. **214**, 503 (2000).
23. M. Martin, J. Photochem. Photobiol. A **66**, 263 (1992).
24. P. S. Skell, L. M. Jackman, S. Ahmed, M. L. McKee, P. B. Shevlin, J. Am. Chem. Soc. **111**, 4422 (1989).
25. X. Gu, Y. Guo, F. Zhang, A. M. Mebel, R. I. Kaiser, Faraday Discuss. **133**, 245 (2006).

26. A. D. Becke, J. Chem. Phys. **98**, 5648 (1993).
27. C. Lee, W. Yang, and R. G. Parr, Phys. Rev. B **37**, 785 (1988).
28. C. Gonzales and H. B. Schlegel, J. Chem. Phys. **90**, 2154 (1989).
29. A. M. Mebel, K. Morokuma, and M. C. Lin, J. Chem. Phys. **103,** 7414 (1995).
30. G. D. Purvis and R. J. Bartlett, J. Chem. Phys. **76**, 1910 (1982).
31. G. E. Scuseria, C. L. Janssen, and H. F. Schaefer, III, J. Chem. Phys. **89**, 7382 (1988).
32. G. E. Scuseria, and H. F. Schaefer, III, J. Chem. Phys. 90, 3700 (1989).
33. J. A. Pople, M. Head-Gordon, and K. Raghavachari, J. Chem. Phys. 87, 5968 (1987).
34. (a) H.-J. Werner, P. J. Knowles, J. Chem. Phys. **82**, 5053 (1985).
35. P. J. Knowles, H.-J. Werner, Chem. Phys. Lett. **115**, 259 (1985).
36. H.-J. Werner, Mol. Phys. **89**, 645 (1996).
37. M. J. Frisch et al., Gaussian 98, Revision A.9; Gaussian, Inc.: Pittsburgh, PA, 1998.
38. MOLPRO is a package of ab initio programs written by H.-J. Werner and P. J. Knowles with contributions from R. D. Amos et al., MOLPRO version 2002.6; University of Birmingham: Birmingham, UK, 2003.
39. DALTON, Release 1.2 (2001), is a molecular electronic structure program written by T. Helgaker, H. J. Aa. Jensen, P. Jørgensen, J. Olsen, K. Ruud, H. Ågren, A. A. Auer, K. L. Bak, V. Bakken, O. Christiansen, S. Coriani, P. Dahle, E. K. Dalskov, T. Enevoldsen, B. Fernandez, C. Hättig, K. Hald, A. Halkier, H. Heiberg, H. Hettema, D. Jonsson, S. Kirpekar, R. Kobayashi, H. Koch, K. V. Mikkelsen, P. Norman, M. J. Packer, T. B. Pedersen, T. A. Ruden, A. Sanchez, T. Saue, S. P. A. Sauer, B. Schimmelpfenning, K. O. Sylvester-Hvid, P. R. Taylor, and O. Vahtras.
40. H. Eyring, S. H. Lin, and S. M. Lin, *Basic Chemical Kinetics*; Wiley, New York, 1980.
41. P. J. Robinson and K. A. Holbrook, *Unimolecular Reactions*; Wiley, New York, 1972.
42. J. I. Steinfield, J. S. Francisco, and W. L. Hase, *Chemical Kinetics and Dynamics*; Prentice Hall, Engelwood Cliffs, NJ, 1999.
43. P. Zhang, S. Irle, K. Morokuma, G. S. Tschumper, J. Chem. Phys. **119**, 6524 (2003).
44. G.-S. Kim, T. L. Nguyen, A. M. Mebel, S. H. Lin, M. T. Nguyen, J. Phys. Chem. A **107**, 1788 (2003).
45. A. M. Mebel, K. Morokuma, M. C. Lin, J. Chem. Phys. **103**, 3440 (1995).
46. Y. Kurosaki, T. Takayanagi, J. Chem. Phys. **113**, 4060 (2000).
47. Le, T. N.; A. M. Mebel, R. I. Kaiser, J. Comput. Chem. **22**, 1522 (2001).
48. R. I. Kaiser, N. Balucani, D. O. Charkin, A. M. Mebel, Chem. Phys. Lett. **382**, 112 (2003).
49. X. Gu, Y. Guo, A. M. Mebel, R. I. Kaiser, J. Phys. Chem. A **110**, 11265 (2006).
50. Y. Guo, V. V. Kislov, X. Gu, F. Zhang, A. M. Mebel, R. I. Kaiser, Astrophys. J. **653**, 1577 (2006).
51. A. M. Mebel, V. V. Kislov, R. I. Kaiser, J. Chem. Phys. **125**, 133113 (2006).
52. A. M. Mebel, R. I. Kaiser, Y. T. Lee, J. Am. Chem. Soc. **122**, 1776 (2000).

53. N. Balucani, A. M. Mebel, Y. T. Lee, R. I. Kaiser, J. Phys. Chem. A **105**, 9813 (2001).
54. X. Gu, Y. Guo, F. Zhang, A. M. Mebel, R. I. Kaiser, Chem. Phys. 335, 95 (2007).
55. N. Hansen, S. J. Klippenstein, C. A. Taatjes, J. A. Miller, J. Wang, T. A. Cool, B. Yang, R. Yang, L. Wei, C. Huang, J. Wang, F. Qi, M. E. Law, P. R. Westmoreland, J. Phys. Chem. A **110**, 3670 (2006).
56. J.-P. Aycard, A. Allouche, M. Cossu, and M. Hillerbrand, J. Phys. Chem. A **103**, 9013 (1999).
57. J. A. Stearns, T. S. Zwier, E. Kraka, D. Cremer, Phys. Chem. Chem. Phys. **8**, 5317 (2006).
58. Y. Hidaka, Int. J. Chem. Kinet. **24**, 871 (1992).
59. A. M. Mebel, V. V. Kislov, R. I. Kaiser, J. Phys. Chem. A **110**, 2421 (2006).
60. A. M. Mebel, S. H. Lin, X. M. Yang, Y. T. Lee, J. Phys. Chem. A **101**, 6781 (1997).
61. T. L. Nguyen, A. M. Mebel, R. I. Kaiser, J. Phys. Chem. A **105**, 3284 (2001).
62. X. Gu, Y. Guo, F. Zhang, A. M. Mebel, R. I. Kaiser, Chem. Phys. Lett. 444, 220 (2007).
63. Y. Guo, X. Gu, F. Zhang, A. M. Mebel, R. I. Kaiser, J. Phys. Chem. A **110**, 10699 (2006).
64. V. V. Kislov, T. L. Nguyen, A. M. Mebel, S. H. Lin, S. C. Smith, J. Chem. Phys. **120**, 7008 (2004).
65. J. A. Miller, Faraday Discuss. **119**, 461 (2001).
66. G. Pascoli, A. Polleux, A.A., 2000, **359**, 799.
67. M. Ohishi, N. Kaifu, Faraday Discuss. **109**, 205 (1998).
68. M. Guelin, S. Green, P. Thaddeus, Astrophys. J. **224**, L27 (1978).
69. M. Cernicharo, C. Kahane, J. Gomez-Gonzalez, M. Guelin, Astron. Astrophys. **164**, L1 (1986).
70. C. M. Walmsley, P. R. Jewell, L. E. Snyder, G. Winnewisser, Astron. Astrophys. **134**, L11 (1984).
71. J. Cernicharo, M. Guelin, K. M. Menten, C. M. Walmsley, Astron. Astrophys. **181**, L1 (1987).
72. M. Guelin, J. Cernicharo, M. J. Travers, M. C. McCarthy, C. A. Gottlieb, P. Thaddeus, M. Ohishi, S. Saito, S. Yamamoto, Astron. Astrophys. **317**, L1 (1997).
73. J. Cernicharo, M. Guelin, Astron. Astrophys. **309**, L27 (1996).
74. C. A. Gottlieb, M. C. McCarthy, M. J. Travers, P. J. Thaddeus, Chem. Phys. **109**, 5433 (1998).
75. T. J. Millar, E. Herbst, Astron. Astrophys. **288**, 561 (1994).